2012

Residential Air-Conditioning System with Smart-Grid Functionality

Auswin George Thomas
Iowa State University

Residential air-conditioning system with smart-grid functionality

by

Auswin George Thomas

A thesis submitted to the graduate faculty

in partial fulfillment of the requirements for the degree of

MASTER OF SCIENCE

Major: Electrical Engineering

Program of Study Committee:

Dionysios Aliprantis, Co-major Professor

Leigh Tesfatsion, Co-major Professor

Umesh Vaidya

Iowa State University

Ames, Iowa

2012

TABLE OF CONTENTS

LIST OF TABLES

LIST OF FIGURES

ACKNOWLEDGMENTS

I would like to thank my major professors Dionysios Aliprantis and Leigh Tesfatsion and God Almighty without whose support I would not have been able to complete this work. I also thank the Electric Power Research Center (EPRC), Pacific Northwest National Laboratory (PNNL) and other agencies that have sponsored this project.

I would like to dedicate this thesis to my parents Joseph Swamidoss Thomas and Thenmozhi Thomas and my brother Godwin Richard Thomas for the unconditional love and support they offered throughtout my course. Last but not the least I need to mention that my friends and colleagues at Iowa State and back in India have been very supportive of me in completing this work.

ABSTRACT

This thesis sets forth a novel intelligent residential air-conditioning (A/C) system controller that provides optimal thermal comfort and electricity cost trade-offs for a household resident based on four key aspects, namely (i) a resident's behavioral preferences, (ii) the structural attributes of the house and the A/C system, (iii) a retail price signal, and (iv) the environmental conditions. It also describes a computational platform that tests the effects of the aggregate intelligent A/C load on the bulk power system. An interesting feedback loop is established between the wholesale power market and the distribution system in that the wholesale energy prices affect the aggregate intelligent A/C load that in turn affects the wholesale energy prices.

CHAPTER 1. GENERAL INTRODUCTION

The U.S. electrical grid is the largest interconnected system on Earth [1]. The grid is expected to face a number of challenges in the future, and intelligent means of tackling them will result in increased reliability and decreased costs. A Massachusetts Institute of Technology (MIT) report [2] outlines some of the major challenges and opportunities that the grid is expected to face in the next decade. These include: inclusion of wind and solar power generation; use of electric vehicles and small-scale distributed electric generation; meeting workforce needs; efficient use of new technologies to deliver high performance and reliability; and capability to handle the increase in data communications within the grid. These concepts belong under the umbrella of a relatively new concept, termed the "smart grid." The smart grid as defined by the DoE [3] refers to a broad class of technology and innovation that aims to integrate the power system with computerized control and automation so as to increase its efficiency, reliability and resiliency.

One of the major functions of the smart grid is to make the grid more energy efficient. Energy efficiency is the ability to reduce the energy usage to deliver the same products and services. The following facts are obtained from [1]:

> "If the grid were just 5% more efficient, the energy savings would equate to permanently eliminating the fuel and greenhouse gas emissions from 53 million cars. If every American household replaced just one incandescent bulb with a compact fluorescent bulb, the country would conserve enough energy to light 3 million homes and save more than $600 million annually." [1, p. 7]

Broadly speaking, the energy efficiency of the entire system can be improved by introducing clean forms of power generation such as wind and solar power generation. They would also

play an important role in reducing the carbon emissions in the future. Increased penetration of distributed generation (DG) such as rooftop photovoltaic generation will serve to reduce the net load in the distribution system while plug-in electic vehicles (PEVs) help in reducing carbon emissions in the transportation sector and storing electrical energy. Conventional load in the grid has remained passive and has to be met under all circumstances. One of the key features of the smart grid is the improved communication between the consumers and the utilities that gives the consumers incentives and flexibility to control their power. This control of load to benefit the power system is termed as demand side management (DSM).

DSM has been practiced since the 80's [4, 5, 6]. In [7], DSM is performed by minimizing the end-user discomfort. [8] discusses the design of utility-consumer contracts for effective DSM. DSM can also be used to provide various services to the power system such as regulation, load shifting, load shaping and peak reduction [9]. [10], [11] and [12] show some of the recent trends in DSM with respect to the smart grid. There are different methods to control the load in DSM [13]: direct load control and indirect load control. In direct control, the power consumption of the consumers is controlled directly by the utility through a control signal. The consumers are contracted by the utility in that their appliances (air conditioners, water heaters, dishwashers, etc.) can be controlled independently by the utilities at any time. This gives less flexibility to the consumer and it also requires high-speed communication infrastructure (e.g., signals from the utility to turn on or turn off the consumer's appliance) to be present. In indirect load control, the power consumption of consumers is controlled either manually by them or with the help of an automatic controller. In this case, the consumer/automatic controller is presented with a control (price) signal that incentivizes the consumer to take appropriate action. A very common control signal is the price of electricity that the consumer is charged. It can also be practically implemented at present as the price signal can be downloaded from the internet by the consumer/automatic controller. In this thesis, the pricing signal is indirectly used to control the load arising from residential consumers (air-conditioning system in particular). The household residents are presented with a time-varying price signal one day in advance in an aim to reduce their air-conditioning system electricity consumption in the present day. This gives them an incentive to reduce their consumption during the peak price hours that reduces their

cost of electricity consumption.

As it is important to reduce the electricity consumption through indirect load control, it is equally important to investigate the effects of this load on the bulk power system. Currently, the market rules and the players in the power system such as generating companies (GenCos) and load serving entities (LSEs) do not deal with active retail load whose implications could be many. Hence, the investigation of the impact of active load in the bulk power system also forms one of the major aspects of this thesis.

1.1 Thesis Organization

This thesis' chapters correspond to one journal and one conference paper that I have co-authored with myself as the lead author.

In Chapter 2, a novel residential air-conditioning (A/C) system controller is presented. This controller is able to provide optimal tradeoffs between the thermal comfort achieved by a resident and the cost he/she pays for his/her A/C usage by taking consumer preferences, structural attributes of the house, retail price signal and environmental conditions into account. An optimization problem is formulated to solve the given task in a resonable amount of time, and simulation results are shown that indicate reduction in the cost of electricity consumption.

As mentioned above, it is desirable to investigate the effects of the price-responsive residential air-conditioning load on the wholesale and retail power system. To accomplish this, Chapter 3 makes of use of a large distribution feeder that has hundreds of households with the intelligent A/C controller described in Chapter 2. The retail load arising from this distribution feeder is fed to the wholesale power system and the effects of this interaction is examined in some detail. The main purpose of Chapter 3 is to develop a framework with which interesting experiments integrating the retail and wholesale power system can be run.

CHAPTER 2. INTELLIGENT RESIDENTIAL AIR-CONDITIONING SYSTEM WITH SMART-GRID FUNCTIONALITY

A paper accepted to be published in the *IEEE Transactions on Smart Grid*

Auswin George Thomas, Pedram Jahangiri, Di Wu, Chengrui Cai,
Huan Zhao, Dionysios C. Aliprantis, and Leigh Tesfatsion

Abstract

This paper sets forth a novel intelligent residential air-conditioning (A/C) system controller that has smart grid functionality. The qualifier "intelligent" means the A/C system has advanced computational capabilities and uses an array of environmental and occupancy parameters in order to provide optimal intertemporal comfort/cost trade-offs for the resident, conditional on anticipated retail energy prices. The term "smart-grid functionality" means that retail energy prices can depend on wholesale energy prices. Simulation studies are used to demonstrate the capabilities of the proposed A/C system controller.

Nomenclature

BR_o	Nominal BTU rating (BTU/h) of the A/C system (at 35° C).
COP_o	Nominal cooling coefficient-of-performance (unit-free) for the A/C system (at 35° C).
C^a	Heat capacity (BTU/°F) of the internal air mass.
C^m	Heat capacity (BTU/°F) of the internal solid mass.
C_n	A/C electricity cost ($) during period n.

$E(\cdot)$	Expected value calculated using $f(\boldsymbol{\nu})$, the probability density function (pdf) for $\boldsymbol{\nu}$.
e_n	Electric energy consumption (kWh) of the A/C system during period n.
$E_n(\cdot)$	Expected value calculated using the marginal pdf for $\boldsymbol{\nu}_n$.
F	Pro-rated fixed cost ($) that the load-serving entity (LSE) charges R for A/C energy usage during each period n.
$f(\boldsymbol{\nu})$	Pdf for $\boldsymbol{\nu} = [\boldsymbol{\nu}_1, \ldots, \boldsymbol{\nu}_N]$.
$G_{\max}$	Maximum possible comfort level (Utils) achievable by house resident R during each period n from the thermal condition of his house.
G_n	Comfort (Utils) attained by R during period n from the thermal condition of his house.
h_1, h_2	Parameters appearing in R's comfort function that weigh R's thermal discomfort for the current and subsequent period, respectively.
I	R's targeted income expenditure level ($).
K	Conversion factor (3412.1 BTU $\approx$ 1 kWh).
k_{1n}, k_{2n}	Lower and upper temperature bounds for R's comfort function in period n.
m^i	Fraction of heat flow rate (unit-free) from internal heat flux to the internal solid mass.
m^l	Fraction of cooling load (unit-free) that indicates the latent cooling load inside the house, i.e., the unwanted moisture that needs to be removed.
m^s	Fraction of heat flow rate (unit-free) from solar radiation to the internal solid mass.
N	Number of successive time periods n comprising R's planning horizon, where period n is defined as the time interval $[(n-1)\Delta t, n\Delta t)$, for some fixed time step Δt.
N_a, N_m	Number of grid points corresponding to T_n^a, T_n^m, respectively.
NB_n	Net benefit (Utils) attained by R in period n (discounted to period 1).
$\mathbf{p}$	Vector of retail A/C energy prices for periods 1 through N, $\mathbf{p} = [p_1, p_2, \ldots, p_N]$.
p_n	Retail price ($/kWh) that the load-serving entity (LSE) charges R for A/C energy

	usage during period n.
$\mathbf{p}^y$	Vector of m consumption good prices, $\mathbf{p}^y = [p_1^y, p_2^y, \ldots, p_m^y]$.
p_j^y	Retail price paid by R per unit of good j.
$\dot{Q}_n$	Heat flow rate (BTU/h) from A/C system to inside air mass during period n.
$\dot{Q}_n^a$	Heat flow rate (BTU/h) from $\dot{Q}_n^s$ and $\dot{Q}_n^i$ to inside air mass during period n.
$\dot{Q}_n^i$	Heat flow rate (BTU/h) from internal appliances and occupants during period n.
$\dot{Q}_n^m$	Heat flow rate (BTU/h) from $\dot{Q}_n^s$ and $\dot{Q}_n^i$ to inside solid mass during period n.
$\dot{Q}_n^s$	Heat flow rate (BTU/h) from solar radiation during period n.
R	The resident of the house.
$\mathbf{r}_n$	Retail price-to-go sequence starting in period n, $\mathbf{r}_n = [p_n, p_{n+1}, \ldots, p_N]$.
TNB	Total net benefit (Utils) attained by R over the planning horizon (discounted to period 1).
T_n^a	Internal air temperature (°F) at the beginning of period n.
T^b	R's bliss temperature, i.e., the inside air temperature (°F) at which R achieves his maximum comfort level.
T_n^m	Internal mass temperature (°F) at the beginning of period n (i.e., the equivalent temperature of the lumped solid mass).
T_n^o	Outside air temperature during period n (°F).
U^a	Thermal conductance (BTU/h/°F) between internal and external air mass defining the thermal envelope of the house.
U^m	Thermal conductance (BTU/h/°F) between the internal air mass and the solid mass.
$\mathbf{u}$	Sequence of A/C status conditions, $\mathbf{u} = [u_1, \ldots, u_N]$.
u_n	A/C system status (e.g., off or on) in period n.
$\mathbf{w}_n$	Vector of forcing terms in period n.
$\mathbf{x}$	Sequence of state vectors, $\mathbf{x} = [\mathbf{x}_1, \ldots, \mathbf{x}_N]$.
$\mathbf{x}_n$	State vector describing the condition of the house at the beginning of period n.
$\mathbf{y}$	Vector of consumption goods purchased by R during periods $1, \ldots, N$ in addition to A/C energy purchases, $\mathbf{y} = [y_1, \ldots, y_m]^T$.

$Z(\mathbf{y})$	Benefit obtained by R from consumption of $\mathbf{y}$.
α	Parameter (Utils/\$) appearing in R's net benefit function that measures the benefit to R of a dollar of income.
β_n	Discount factor for R's net benefit in period n.
γ	Parameter appearing in R's comfort function that influences the shape of this function around a bliss temperature range.
$\boldsymbol{\nu}$	Sequence of stochastic environmental conditions, $\boldsymbol{\nu} = [\boldsymbol{\nu}_1, \ldots, \boldsymbol{\nu}_N]$.
$\boldsymbol{\nu}_n$	Vector of stochastic (external and internal) environmental conditions during period n.
ρ_n^o	Outside relative humidity during period n.

2.1 Introduction

This study considers the design of a residential air-conditioning (A/C) system capable of responding intelligently to price signals in order to achieve optimal inter-temporal comfort/cost trade-offs for a house resident. A key motivation for this study is a 2010 report by the United States Federal Energy Regulatory Commission (FERC) on demand response and advanced metering technology. This report concludes:

> "The investments in devices, controls and software to implement demand response remain one of the greatest barriers to increased penetration." [14, p. 56]

In line with this conclusion, the current paper carefully considers the complex interplay between the comfort/cost preferences of a house resident and the structural conditions constraining his A/C choices arising both from the physics of energy flows and the engineering limitations of A/C system implementations.

Previous research on comfort and energy management issues has largely focused on large building environments with many occupants [15, 16, 17, 18]. As detailed in the 2009 survey by Dounis and Caraiscos [19], these studies consider not only heating and cooling systems but also other building design features such as window placements, window shading, mechanical ventilation systems, and lighting systems. Occupant comfort in these studies is typically a

complex multi-faceted concept encompassing thermal comfort, visual comfort, and indoor air quality, in keeping with ASHRAE standards [20]. Various control methods are explored in these studies, including fuzzy controllers [21], fuzzy adaptive controllers [17, 22], and neural network controllers [23].

Nevertheless, in recent years the increasing interest in advanced metering infrastructure for households has encouraged researchers to focus more carefully on the energy usage choices of residential homeowners [24]. For example, Rogers et al. [25] study an interesting residential demand model, although without consideration of price signals. Guttromson et al. [26] and Chassin et al. [27] focus on the modeling of price-responsive residential demands constrained by internal and external state conditions. The latter studies are anchored by an Olympic Penninsula pilot project [28]. However, residential energy demands in these studies are modeled by means of pre-specified behavioral rules rather than as the solutions to residential optimization problems. More recent research has set forth formulations of the residential A/C control problem as an optimization problem. In this work the objective is to minimize some combination of thermal discomfort and energy usage under varying electricity prices [29, 30, 31, 32, 33].

The current paper extends this prior work in three important directions. First, the A/C control strategy is formulated as a stochastic dynamic program in a manner that permits the controller to respond to both energy prices and randomly varying environmental conditions. We demonstrate that the underlying optimization problem can be solved in a reasonable amount of time using conventional computational resources by adopting a certainty equivalence approach, using weather forecast information that is nowadays readily available over the Internet. Moreover, this is done in a way that is minimally disruptive to the A/C system hardware, which is important for retrofitting existing residential A/C systems. Second, the thermal dynamics for the house and the A/C system are represented by means of physics-based models that are suitably realistic for residential A/C system control purposes (whereas previous work adopted simpler models to describe the plant dynamics). Third, the objective function expressing comfort/cost trade-offs for the household resident is rigorously motivated in terms of basic economic principles.

Section 2.2 sets out the stochastic optimal control problem in general terms: a residential A/C system determines energy usages over an N-period planning horizon to achieve optimal intertemporal comfort/cost trade-offs for the house resident, conditional on anticipated energy prices and on dynamically changing internal and external conditions. In this general formulation it is assumed that reliable state equations are available for determining the change in the thermal state of the resident's house from one period to the next as a function of the resident's A/C energy usage level and environmental parameters. It is also assumed that the resident's comfort level is determined in each period by the indoor thermal state of his house at the beginning and end of the period.

Sections 2.3 and 2.4 then address what might be done in the more practically relevant case in which the state equations for the resident's house must be approximated and the resident's achievable comfort levels are constrained by the mechanical requirements of the resident's A/C system. Illustrative findings from computer simulations demonstrating the capabilities of the resulting A/C system controller are reported in Section 2.5. Concluding remarks are given in Section 2.6. Appendix 2.7.1 provides technical details regarding the use of a Luenberger observer to construct an estimate for mass temperature, and Appendix 2.7.2 provides additional motivation for the modeling of the resident's comfort/cost trade-offs.

2.2 General Stochastic Optimal Control Problem for a Residential A/C System

2.2.1 Problem Formulation

For computational tractability, the planning horizon of the house resident is discretized into time periods $n = 1, \ldots, N$, and the continuous thermal dynamics of the house are correspondingly discretized into the discrete-time motion of a state vector $\mathbf{x}_n$. However, the dimension and content of the state vectors $\mathbf{x}_n$ are not restricted. Consequently, the state equation formulation in this section is generic and can be used to implement a wide variety of thermal models.[1]

[1] In Section 2.3, below, this generic formulation is concretely illustrated for a thermal model with two-dimensional state vectors $\mathbf{x}_n$, where the two state components are internal air temperature T_n^a and internal solid mass temperature T_n^m.

The state $\mathbf{x}_{n+1}$ is assumed to be determined as a function S_n (time-varying for generality) of the previous state $\mathbf{x}_n$, the A/C status u_n, and a vector $\boldsymbol{\nu}_n$ of environmental parameters, as

$$\mathbf{x}_{n+1} = S_n(\mathbf{x}_n, u_n, \boldsymbol{\nu}_n) \ , \quad n = 1, \ldots, N \ , \tag{2.1}$$

where the initial state at the beginning of period 1 is exogenously given as

$$\mathbf{x}_1 = \overline{\mathbf{x}}_1 \, . \tag{2.2}$$

The A/C status u_n in (2.1) is assumed to be restricted to a domain U. For example, $U = \{-1, 0\}$ could represent a bang-bang control domain corresponding to cooling and off, whereas $U = [-1, 0]$ could represent a continuous control domain ranging from full cooling (-1) to off (0). Also, suppose the A/C heat flow rate $\dot{Q}_n$ is determined as a function

$$\dot{Q}_n = \dot{Q}(u_n, \boldsymbol{\nu}_n) \, . \tag{2.3}$$

Finally, assume the electric energy usage e_n of the A/C system can be expressed as a function

$$e_n = e(\dot{Q}_n, \boldsymbol{\nu}_n) \equiv \tilde{e}(u_n, \boldsymbol{\nu}_n) \, . \tag{2.4}$$

To model price-responsive demand for electricity, it is assumed that resident R has a retail contract with a load-serving entity (LSE) under which he pays a price p_n (\$/kWh) for his A/C energy usage e_n (kWh) plus a pro-rated fixed charge F (\$) to cover costs such as equipment purchases and connection fees.[2] The total cost charged by the LSE to R during period n thus takes the form

$$C_n = C(p_n, e_n) = p_n e_n + F \, . \tag{2.5}$$

The sequence $\mathbf{p} = [p_1, p_2, \ldots, p_N]$ of retail A/C energy prices is assumed to be communicated by the LSE to R prior to the start of period 1. Although R has access to this price data, he does not need to act on a continual basis. Rather, it is the intelligent A/C controller that assumes

[2] In the general problem formulation presented in this section, the manner in which the LSE sets the A/C energy usage prices p_n is not restricted; hence, in particular, these prices do not need to bear any particular relationship to the prices paid by the LSE for its wholesale energy purchases. In reality, of course, an LSE that contracts with retail consumers having intelligent A/C system controllers as modeled in the current study will have to set its A/C energy usage prices in line with the prices it pays for energy at wholesale in order to remain profitable. For example, as illustrated below in Section 2.5, p_n could be set equal to the day-ahead locational marginal price (LMP) paid by the LSE at wholesale plus a "mark-up" to cover additional types of operational costs.

this responsibility. Note that the time step of the A/C system model does not have to be the same as the time step of operations for the wholesale electric power market. For example, day-ahead market LMPs are determined on an hourly basis in the United States whereas an A/C system will typically run at a faster time rate. If hourly day-ahead market LMPs were to be charged to R as retail energy prices, the vector $\mathbf{p}$ would consist of 24 equal-length sub-vectors of constant-valued prices.

As in [25], the comfort level (Utils) attained by R in period n from the thermal condition of his house is measured as a time-varying function of the state vectors at the beginning and end of period n:

$$G_n = G(\mathbf{x}_n, \mathbf{x}_{n+1}, n)\,. \tag{2.6}$$

As is standard in (power) economics, the comfort assessment (2.6) is assumed to be determined independently of any cost considerations.

From the viewpoint of period 1, the net benefit NB_n attained by R in period n is given by R's attained comfort level minus his energy purchase costs, weighted by a discount factor β_n, as follows:

$$\mathrm{NB}_n = \beta_n[G(\mathbf{x}_n, \mathbf{x}_{n+1}, n) - \alpha C(p_n, \tilde{e}(u_n, \boldsymbol{\nu}_n))]\,. \tag{2.7}$$

The key parameter α (Utils/\$) appearing in (2.7) measures the benefit (utility) to R of an additional dollar of income. It permits costs measured in dollars to be expressed in benefit units (Utils), so that comfort/cost trade-offs can be calculated.

The precise sense in which α quantifies the trade-off between comfort satisfaction and energy cost for R is explained in some detail in Appendix 2.7.2 of our paper. Specifically, it is shown in Appendix 2.7.2 that α can be derived as the shadow price for R's budget constraint in a more fully articulated constrained benefit maximization problem: namely, the maximization of R's benefit from consumption of multiple goods/services (including thermal comfort) subject to a budget constraint. Thus, α measures R's "marginal benefit of income" at the optimization point, i.e., the drop in the maximized value of R's benefit that would result if R had one less dollar of income to spend (e.g., due to a higher energy price). For simplicity, this section treats a reduced form of this more comprehensive benefit maximization problem in which R is in

effect solving a first-order necessary condition for this more comprehensive problem, taking α as given.[3]

The total net benefit attained by R over the planning horizon from period 1 to period N, conditional on a given state sequence $\mathbf{x}$, A/C status sequence $\mathbf{u}$, environmental-term sequence $\boldsymbol{\nu}$, and price sequence $\mathbf{p}$ is calculated as the discounted sum of period-by-period net benefits:

$$\mathrm{TNB}(\mathbf{x}, \mathbf{u}, \boldsymbol{\nu}, \mathbf{p}) = \Sigma_{n=1}^{N} \mathrm{NB}_n \,. \tag{2.8}$$

Let the expected value of (2.8), conditional on (2.1) through (2.7), be denoted by

$$E[\mathrm{TNB}(\mathbf{x}, \mathbf{u}, \boldsymbol{\nu}, \mathbf{p})] = \int_V \mathrm{TNB}(\mathbf{x}, \mathbf{u}, \boldsymbol{\nu}, \mathbf{p}) f(\boldsymbol{\nu}) d\boldsymbol{\nu} \tag{2.9}$$

where V denotes the domain of possible environmental vectors $\boldsymbol{\nu}$ that could be realized during the planning horizon $\{1, \ldots, N\}$, and $f(\boldsymbol{\nu})$ denotes the joint probability density function (PDF) for $\boldsymbol{\nu}$.

Putting this all together, the stochastic optimal control problem to be solved at the beginning of period 1 for determination of optimal A/C status choices $u_n^* \in U$ during periods $n = 1, \ldots, N$ can be expressed as follows:

$$\max E[\mathrm{TNB}(\mathbf{x}, \mathbf{u}, \boldsymbol{\nu}, \mathbf{p})] \tag{2.10}$$

with respect to $\mathbf{u} = [u_1, u_2, \ldots, u_N]^T$ subject to (2.1) and (2.2).

2.2.2 Closed-Loop Dynamic Programming Solution

Stochastic dynamic programming can be used to solve the control problem (2.10) in closed-loop form. That is, (2.10) can be solved in sequential form with the optimal A/C status value $u_n^*(\mathbf{x}_n; \mathbf{r}_n)$ in each period n expressed as a function of the current state $\mathbf{x}_n$, conditional on the price-to-go sequence $\mathbf{r}_n = [p_n, p_{n+1}, \ldots, p_N]^T$ consisting of the given retail energy prices from period n through the final planning period N. For any n satisfying $1 \leq n \leq N$, let $\mathrm{Val}_n(\mathbf{x}_n; \mathbf{r}_n)$ denote the maximum expected total net benefits attainable by R starting from

[3] As a practical matter, a household resident could experiment with different α values to find a value for this trade-off parameter that approximately reflects his true marginal benefit of income.

any feasible state $\mathbf{x}_n$, conditional on $\mathbf{r}_n$. That is, let $\text{Val}_n(\mathbf{x}_n;\mathbf{r}_n)$ denote R's price-conditioned *period-n value function.*[4]

From the developments in Section 2.2.1, we can define

$$\text{Val}_N(\mathbf{x}_N;\mathbf{r}_N) = \max_{u_N} E_N[\text{NB}_N(\mathbf{x}_N, S_N(\mathbf{x}_N, u_N, \boldsymbol{\nu}_N), p_N, \tilde{e}(u_N, \boldsymbol{\nu}_N))] \tag{2.11}$$

where $\mathbf{r}_N \equiv p_N$ denotes the retail energy price for period N, and the expectation is taken with respect to the randomly varying environmental conditions $\boldsymbol{\nu}_N$ for period N, conditional on $\mathbf{x}_N$ and exogenously given factors (such as $\mathbf{r}_N$). Note that the solution to (2.11) has the closed-loop form $u_N^* = u_N(\mathbf{x}_N;\mathbf{r}_N)$. It then follows, by definition, that resident R's value functions satisfy the following recursive relationship:[5] For $n = 1, \ldots, N-1$:

$$\begin{aligned}\text{Val}_n(\mathbf{x}_n;\mathbf{r}_n) = \max_{u_n} E_n[&\text{NB}_n(\mathbf{x}_n, S_n(\mathbf{x}_n, u_n, \boldsymbol{\nu}_n), p_n, \tilde{e}(u_n, \boldsymbol{\nu}_n)) \\ &+ \text{Val}_{n+1}(S_n(\mathbf{x}_n, u_n, \boldsymbol{\nu}_n);\mathbf{r}_{n+1})]\,.\end{aligned} \tag{2.12}$$

where $\mathbf{r}_n \equiv [p_n, \mathbf{r}_{n+1}]$.

Consequently, in principle, resident R at the beginning of period 1 can derive a closed-loop solution to his stochastic optimal control problem (2.10) as follows. He should first use (2.11) and (2.12) to derive his value functions $\text{Val}_n(\mathbf{x}_n;\mathbf{r}_n)$, starting at period $n = N$ and working backward to period $n = 1$. As a by-product of these calculations, for each period $n \geq 1$ the resident will obtain the optimal A/C status choice $u_n^*(\mathbf{x}_n;\mathbf{r}_n)$ as a function of $\mathbf{x}_n$, conditional on $\mathbf{r}_n$.

From the vantage point of the initial period, R does not yet know what state vectors $\mathbf{x}_n$ will be realized in subsequent periods due to the inherent uncertainty in the system. Nevertheless, he will know $\mathbf{x}_n$ at the beginning of each period n prior to his actual choice of an A/C status u_n. The closed-loop solutions $u_n^*(\mathbf{x}_n;\mathbf{r}_n)$ are thus complete contingency plans determining what A/C status choice should be optimally implemented at each future time, conditional on the state and price conditions at that time. Clearly, however, the state domain would have to be appropriately discretized to obtain a practically computable closed-loop solution. An example of such a discretization is provided in Section 2.4.

[4] The exogenously given price-to-go sequences $\mathbf{r}_n$ are explicitly included as conditioning factors in the optimal control and value functions in order to emphasize the price-responsive nature of the A/C system controller.

[5] Equation (2.12) is a special case of Bellman's Principle of Optimality.

2.3 Physics-Based Modeling of the A/C System

The A/C system is a conventional residential system, such as the ones that may be typically found in United States middle-class residences. These are conventional systems, with an electrically powered central unit or a window/wall unit that cycles on and off to maintain the air temperature around a thermostat set point. This section provides explicit forms for the abstractly represented thermal state equation (2.1) and energy equation (2.4), as foundations for the proposed intelligent A/C system controller. The complexity of these forms arises because they are physically based. An important point here, however, is that house residents employing the proposed controller do not need to be exposed to this complexity; an interface can separate a resident from the internal workings of the controller. As will be clarified more carefully in Section 2.4 below, all that a resident needs to be exposed to via this interface are "knobs" permitting him to adjust to his satisfaction the settings for his thermal comfort function parameters and his comfort/cost trade-off parameter α.

The thermal dynamics for a house are represented by means of an Equivalent Thermal Parameter (ETP) model [34, 35]. The ETP model supposes that the state of a house at time t consists of the inside air and mass temperatures, T^a and T^m, whose dynamics are defined by a system of two first-order linear differential equations:

$$\frac{dT^a}{dt} = \frac{1}{C^a}\left[(T^o - T^a)U^a + (T^m - T^a)U^m + \dot{Q} + \dot{Q}^a\right] \tag{2.13}$$

$$\frac{dT^m}{dt} = \frac{1}{C^m}\left[(T^a - T^m)U^m + \dot{Q}^m\right] . \tag{2.14}$$

The parameters appearing above have been defined in the nomenclature; also

$$\dot{Q}^a = (1 - m^s)\dot{Q}^s + (1 - m^i)\dot{Q}^i \tag{2.15}$$

$$\dot{Q}^m = m^s\dot{Q}^s + m^i\dot{Q}^i . \tag{2.16}$$

For computational tractability, the above continuous-time system is transformed to a discrete-time system of the form

$$\mathbf{x}_{n+1} = \hat{\mathbf{A}}\mathbf{x}_n + \hat{\mathbf{B}}\mathbf{w}_n \tag{2.17}$$

under the assumption that all time-varying forcing terms are step functions that remain constant

during each period n, with

$$\mathbf{w}_n = \begin{bmatrix} T_n^o & \dot{Q}_n^s & \dot{Q}_n^i & \dot{Q}_n \end{bmatrix}^T . \tag{2.18}$$

This discrete state equation is of the same form as (2.1). To see this, first note that the A/C heat flow rate $\dot{Q}_n$ depends on the A/C status u_n (cooling or off), which is represented by the following indicator function:

$$u_n = \begin{cases} 0 & \text{if A/C status = off} \\ -1 & \text{if A/C status = on} \end{cases} \tag{2.19}$$

The A/C heat flow rate $\dot{Q}_n$ represented by (2.3) is defined as

$$\dot{Q}_n = \dot{Q}(u_n, \boldsymbol{\nu}_n) = \frac{\mathrm{BR}(T_n^o)}{m(\rho_n^o)} u_n \tag{2.20}$$

where the vector $\boldsymbol{\nu}_n$ contains all stochastic time-varying terms,

$$\boldsymbol{\nu}_n = \begin{bmatrix} T_n^o & \dot{Q}_n^s & \dot{Q}_n^i & \rho_n^o \end{bmatrix}^T . \tag{2.21}$$

In particular, the state function S_n in (2.1) reduces to a time-invariant function S of $(\mathbf{x}_n, u_n, \boldsymbol{\nu}_n)$ that is linear in $\mathbf{x}_n$.

Finally, an explicit form for the energy consumption function (2.4) of the A/C is established as

$$e_n = e(\dot{Q}_n, \boldsymbol{\nu}_n) = K \frac{|\dot{Q}_n|}{\mathrm{COP}(\boldsymbol{\nu}_n)} m(\rho_n^o) \Delta t \, . \tag{2.22}$$

Explicit numerical expressions for the functions that appear above are obtained from [35]:

$$\mathrm{BR}(T_n^o) = \mathrm{BR_o} \left(1.4892 - 0.0052 T_n^o\right) \tag{2.23}$$

$$\mathrm{COP}(\boldsymbol{\nu}_n) = \frac{\mathrm{COP_o}}{-0.01364 + 0.01067 T_n^o} \tag{2.24}$$

$$m(\rho_n^o) = 1.1 + \frac{m^l}{1 + \exp(4 - 0.1\rho_n^o)} \, . \tag{2.25}$$

2.4 Controller Implementation

This section explains the envisioned practical implementation of the proposed intelligent A/C system controller, given the A/C system model described in Section 2.3. This controller

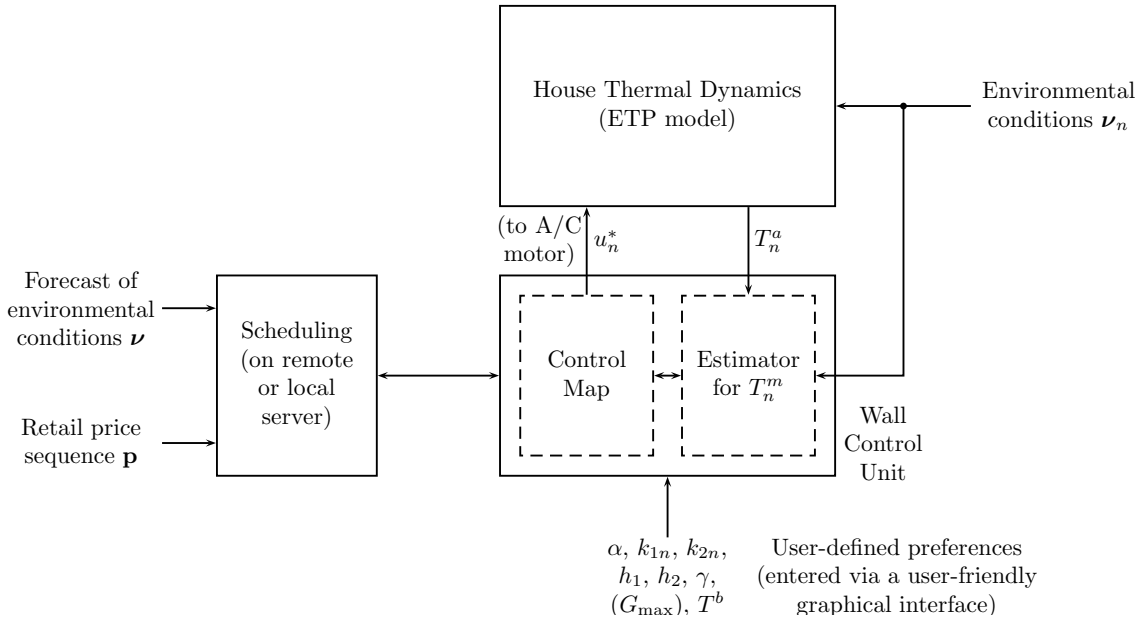

Figure 2.1 Block-diagram schematic of the intelligent A/C system control.

consists of two main parts, namely, the software running the scheduling algorithm and the wall control unit, as shown in Fig. 2.1.

Current residential A/C systems, whose logic is based on relatively simple thermostatic control, could be readily retrofitted by just upgrading their wall control units with the proposed intelligent unit (i.e., the A/C mechanical components would not need to be modified). The scheduling software could be programmed on the actual wall control unit; alternatively, in order to reduce hardware cost, it could run on a remote server as a cloud computing application, managed by an entity offering this service. The wall control unit also requires communications capability, for example, a wireless connection to the house's broadband internet.

At the time of installation, the four thermal parameters of the ETP model, namely C^a, C^m, U^a, and U^m, would have to be programmed into the unit, since they are required for the model-based optimization process. These, together with m^i and m^s, may be determined using a standard spreadsheet-like calculation process based on the physical dimensions of the house such as the number of stories, the number and orientation of windows and doors, the floor area, and the level of thermal insulation[36]. The installer also would need to enter the BR and COP functions of the A/C unit.

For R's thermal comfort function, we adopt the following simple representation loosely based on the ANSI/ASHRAE 55-2010 standard [20] and similar to the one used in [25]:

$$G_n = G(\mathbf{x}_n, \mathbf{x}_{n+1}, n) = G_{\max} - h_1 f(\mathbf{x}_{n,1}, n) - h_2 f(\mathbf{x}_{n+1,1}, n+1)\,, \tag{2.26}$$

where the function f is defined as

$$f(x,n) = \begin{cases} [x - (T^b - k_{1n})]^\gamma & \text{if } x < T^b - k_{1n} \\ [x - (T^b + k_{2n})]^\gamma & \text{if } x > T^b + k_{2n} \\ 0 & \text{otherwise} \end{cases} \tag{2.27}$$

The parameters h_1, h_2, k_{1n}, and k_{2n} are positive constants, whereas γ is a positive even integer. An increase in γ increases the magnitude of the slope of the discomfort function f when moving away from the bliss temperature range.[6]

This modeling of R's comfort function can be interpreted as follows. For periods n during which the house resident R is at home, he can set $k_{1n} = k_{2n} = 0$, so that he attains his maximum comfort level when the air temperature (the first element of $\mathbf{x}_n$) is maintained at his bliss temperature. When the resident is not at home, nonzero values for k_{1n} and k_{2n} can be set, so that the same comfort level is attained within a range of temperatures, $T^b - k_{1n}$ and $T^b + k_{2n}$. In other words, the resident, while absent, is indifferent to the actual temperature inside the house, as long as it stays within the pre-specified range (for instance, to protect pets, foodstuff, or medicinal supplies). It should be noted that R could also decide to have nonzero k_{1n} and k_{2n} set-points even while at home, if this is his preference. The choice of constant representing the maximum comfort level attained ($G_{\max}$) is not of any practical significance, since it does not affect the result of the optimization. Its numerical value can be selected so that R's total net benefit has a positive value, measured in Utils, although this is not critical.

The resident R could program his comfort and cost preferences either directly on the wall control unit or (more realistically) via a user-friendly graphical user interface, which could run

[6] The thermal comfort parameters h_1, h_2, and γ could be modeled as time varying without any technical difficulty. However, R's thermal comfort function (2.26) is meant to measure the true comfort (benefit) that R attains from the thermal state of his house under different thermal and occupancy conditions, independently of cost considerations. A change in the values of these parameters over time would therefore have to reflect some type of time variation in R's basic preferences for thermal comfort. This does not seem reasonable for the relatively short planning interval (one or two days) that we have in mind for the problem formulation.

on R's personal computer, smart phone, or some other mobile computing device. The latter would allow R to program the device without directly entering numerical values; these would be determined internally by the software. The parameters reflecting R's preferences are communicated to the scheduling program. Whenever R decides to modify his bliss temperature or some other parameter, the updated parameter set would be re-sent, and the optimal scheduling would have to be recomputed. The scheduling algorithm also needs the day-ahead price sequence $\mathbf{p}$ and a forecast of future environmental conditions included in vector $\boldsymbol{\nu}$. In particular, it is quite challenging to obtain an accurate forecast of the internal heat flow rate $\dot{Q}_n^i$, which arises from various sources such as people, lights, and electrical appliances. Therefore, a typical variation of this term must be assumed, for example, using the recommendations of [37]. Nevertheless, R might be willing to provide some additional information, such as the number of occupants and relevant details of their daily occupancy schedule, or whether visitors are expected on a certain date/time, which would help improve the scheduling.

Proper discretization of the state vector $\mathbf{x}_n$ is necessary for computational tractability when solving the scheduling problem. The internal air temperature is assumed to vary in the range $[T^b-24, T^b+24]$. To obtain reasonable accuracy, the range is discretized using $N_a = 481$ points, yielding an accuracy of 0.1 °F. The internal mass temperature is discretized with N_m points. Generally, the difference between T_n^a and T_n^m will be small. Herein, it is assumed that T_n^m lies in $[T_n^a - 4.8, T_n^a + 4.8]$, and that $N_m = 481$, yielding an accuracy of 0.02 °F for the difference $(T_n^a - T_n^m)$. A grid has thus been formed containing all allowable combinations of (T_n^a, T_n^m). When applying equation (2.17) during the dynamic programming algorithm, the states obtained are not guaranteed to lie on the grid, so they are moved to their nearest grid point, as illustrated in Fig. 2.2. This prevents the gradual increase of the grid size as dynamic programming proceeds backwards in time. Equations (2.11) and (2.12) are then used to develop the control map for the entire planning horizon. The control map is an $(N_a N_m) \times N$ matrix containing zeros or ones, where each element represents an on-or-off solution of (2.12). For instance, in this implementation, the computer memory required to store this map in binary format (using one bit for each element) is approximately 40 MB, or as low as 2 MB if sparse-matrix storage techniques are used. The dynamic programming algorithm was programmed in Matlab, and

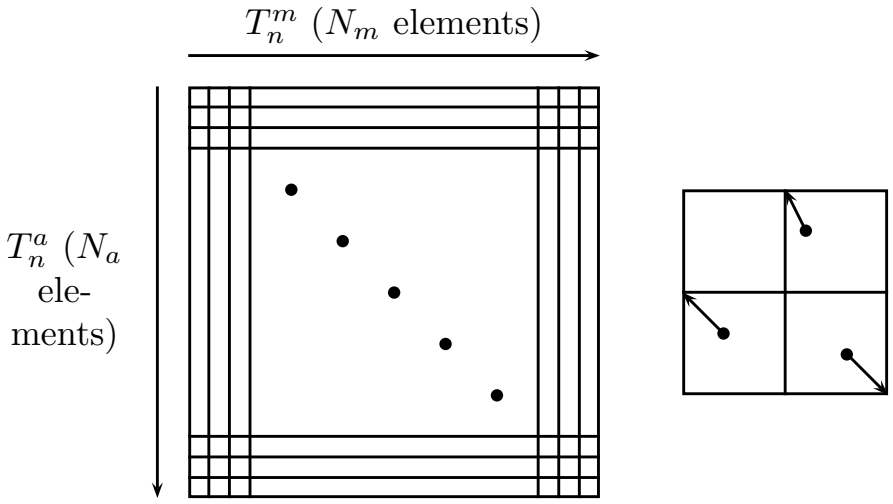

Figure 2.2 Discretization of the state vector $\mathbf{x}_n$.

takes ca. 40 seconds to run on an Intel Core 2 Duo CPU E8400 3-GHz processor with 4 GB of RAM.

It should be noted that the internal mass temperature T_n^m cannot be obtained by direct measurement. However, as demonstrated in Appendix 2.7.1, a Luenberger observer can be designed to estimate it using measurements of the environmental variables (and reasonable assumptions for the internal heat flow rate). These measurements could be obtained by actual temperature, solar irradiation, and humidity sensors installed at the house, or indirectly from weather monitoring websites.

2.5 Simulation Results

This section reports simulation findings for the proposed intelligent A/C system controller. These simulation findings indicate that the controller works as expected to provide a flexible way for a house resident to optimally trade off thermal comfort against costs over time, conditional on his preferences for comfort, his anticipated occupancy times, and his A/C energy usage costs.

As discussed in Section 2.2.1 and Appendix 2.7.2, the α parameter appearing in resident R's net benefit function (2.7) is an attribute of R reflecting his marginal benefit of income, not a control variable. Previous studies have not paid attention to the key role played by

this attribute parameter in the determination of optimal comfort/cost trade-offs for household residents. Consequently, the simulations reported in this section explore outcomes for a range of possible α values for R.

Other parameter values are set as follows. The thermal comfort parameter values for R are set at $G_{\max} = 1.5$ Utils, $h_1 = h_2 = 0.04$ Utils/(°F)^2, $\gamma = 2$, and $T^b = 74$ °F. The thermal model parameter values for R's house are set at $C^a = 794.5$ BTU/°F, $C^m = 4726.4$ BTU/°F, $U^a = 444.3$ BTU/h/°F, $U^m = 7501$ BTU/h/°F, $m^s = m^i = 0.5$, $\mathrm{BR_o} = 42000$ BTU/h, $\mathrm{COP_o} = 3.8$, and $m^l = 0.3$. These were obtained for a hypothetical 1500 ft^2 single-story house with very good insulation.

Meteorological data are obtained from the typical meteorological year (TMY2) database [38], which contains records of a typical year for most of the regions in the United States. A relatively hot day is simulated based on the data corresponding to June 14th, 2009 in Detroit, Michigan. The data are smoothed to represent actual weather conditions and an offset is added to the temperature data. The day-ahead scheduling is carried out based on the outside temperature and relative humidity of the modified data as the forecast.

For the simulation of the A/C system, artificial conditions are synthesized based on the modified TMY2 data. To this end, a small perturbation is superimposed on the modified data to simulate actual (different than forecasted) conditions. The solar radiation incident on the house is a function of the direct normal radiation and the diffuse horizontal radiation. The solar heat gain factor [35] is then used to calculate the heat flow rate from the solar radiation. Radiation data are obtained from the TMY2 file; however, since these are provided on an hourly time-scale, other higher-frequency recorded data from NREL [39] are used to simulate cloud movement in a more realistic fashion.

A crudely predetermined schedule of appliances (based on the design value of internal heat flow rate [35]) is used to construct the internal heat flow rate for the day-ahead scheduling. A finer variation of appliances and occupant activity is assumed to occur in the simulation. The variation of all environmental parameters used for day-ahead scheduling and in simulations is depicted in Fig. 2.3. For scheduling, the variables are represented by piecewise constant functions, changing every hour.

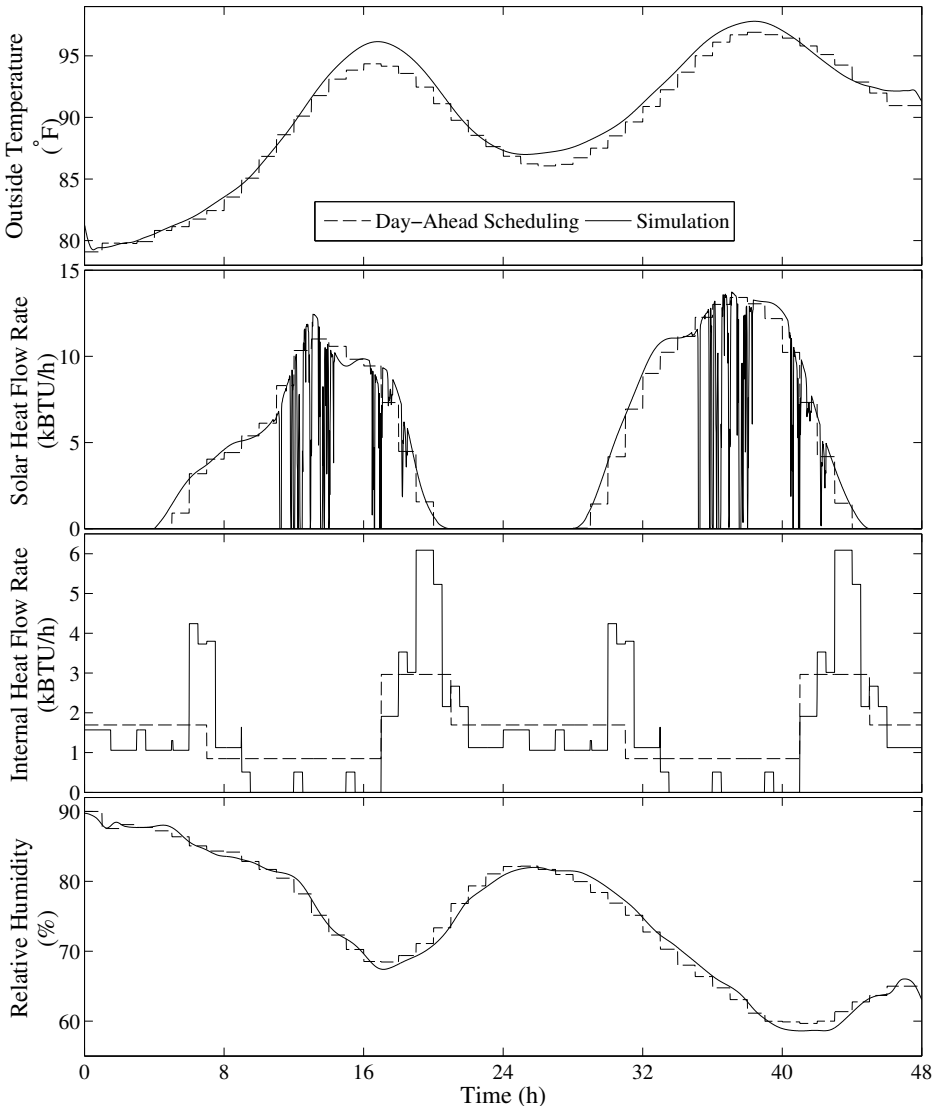

Figure 2.3 Variation of environmental parameters for day-ahead scheduling and simulation.

The retail price corresponding to the chosen region (Detroit, MI) is the day-ahead LMP obtained from an historical LMP report [40] for the Midwest ISO. The price p_n in (2.5) includes the LMP plus a mark-up of 5 cents/kWh, whereas $F = 0$. The retail price variation is shown in Fig. 2.4.

Simulations are run using a 2-day planning horizon, where each period Δt is 2 minutes long (implying $N = 1440$). The discount factors β_n in (2.7) are specified to be 1.0 for the first day of the planning horizon and 0.9 for the second day of the planning horizon.

The general A/C controller set out in Section 2.2.1 postulates the existence of a joint PDF

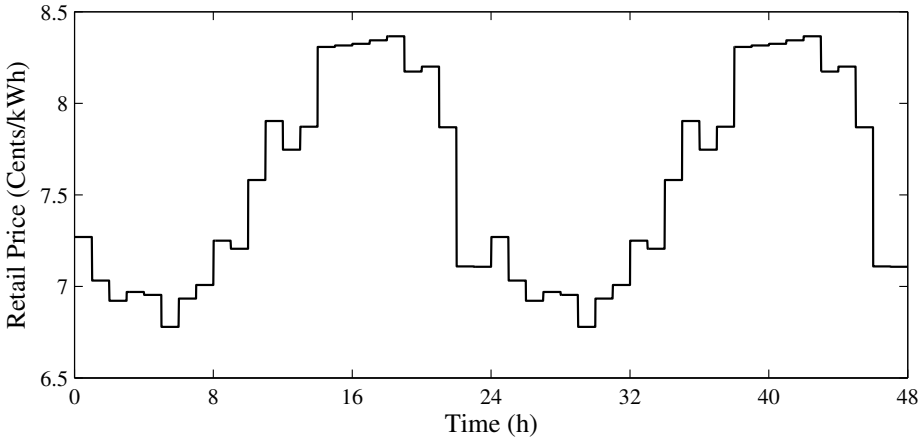

Figure 2.4 Retail price variation.

for the environmental variables over the planning horizon. Nevertheless, for implementation purposes, it would generally be very difficult to obtain or estimate such a joint PDF. Here we make use of a "certainty equivalence" approach to derive an approximate solution for the optimal on/off A/C controls. This approach replaces the random environmental variables over the planning horizon by their expected values, reducing the problem to a deterministic dynamic programming problem. Since the application at hand involves only a short two-day planning horizon, the approximate solution should be reasonably close to the optimal solution.

A few simplifications are introduced to ease the presentation of results. First, because day-ahead LMPs cannot be known with certainty two days in advance, it is assumed that the price sequence for the second day of the planning horizon is forecasted to be the same as for the first day. Second, although a new optimization takes place at the end of each day for a two-day planning horizon, optimization outcomes are only shown for the first 24 hours of each two-day planning horizon.

Finally, it should be noted that the two-day rolling-horizon optimization implemented for the application at hand to generate updates to the A/C control map could instead be undertaken at shorter intervals (e.g., hourly). A shorter rolling-horizon specification would presumably permit a greater forecast accuracy for the environmental variables and improved comfort/cost optimization outcomes, but at the cost of increased computational time.

Table 2.1 Results with $k_{1n} = k_{2n} = 0$

α	24-hour Electricity Cost ($)	24-hour Thermal Comfort (Utils)	24-hour Net Benefit (Utils)	24-hour Energy (kWh)
N/A	2.14	1078.8	N/A	27.3
0	2.14	1072.4	1072.4	27.4
50	2.13	1070.7	964.1	27.3
200	2.11	1064.3	641.8	27.0
500	2.09	1052.7	9.7	26.7
1000	2.04	1016.3	-1026.6	26.2
2000	1.88	862.7	-2888.8	24.1
3000	1.77	675.0	-4624.6	22.7
4000	1.70	429.7	-6374.5	22.0

2.5.1 Resident Stays at Home Throughout the Day

As a first case study, the resident is assumed to remain at home throughout the day, maintaining a constant bliss temperature, and $k_{1n} = k_{2n} = 0$. For comparison purposes, a simulation was first run over a 24-hour horizon using a classical A/C thermostat operating with simple hysteresis control, with a deadband of ± 0.25 °F. The thermal comfort obtained was 1078.8 Utils. (The ideal daily thermal comfort is $(N/2)G_{\max} = 1080$ Utils.) The energy consumption of the A/C system was 27.3 kWh and the electricity cost was $2.14. These results are listed as the first row of Table 2.1 for the reader's convenience.

Fig. 2.5 shows the variation of the indoor air temperature inside R's house for a range of α values. It is obvious that, as α is increased, the deviations of T_n^a from T^b become increasingly prominent. Table 2.1 summarizes the results. As expected, an increase in α results in increased electric energy savings but lower thermal comfort.

2.5.2 Resident Leaves Home During the Day

For the second case study, the resident is assumed to leave the house from 8 am to 5 pm. During this time, k_{1n} and k_{2n} are set to 15 °F. The simulation results shown in Fig. 2.6 exhibit a markedly different pattern from the previous case study. Most notably, the A/C controller

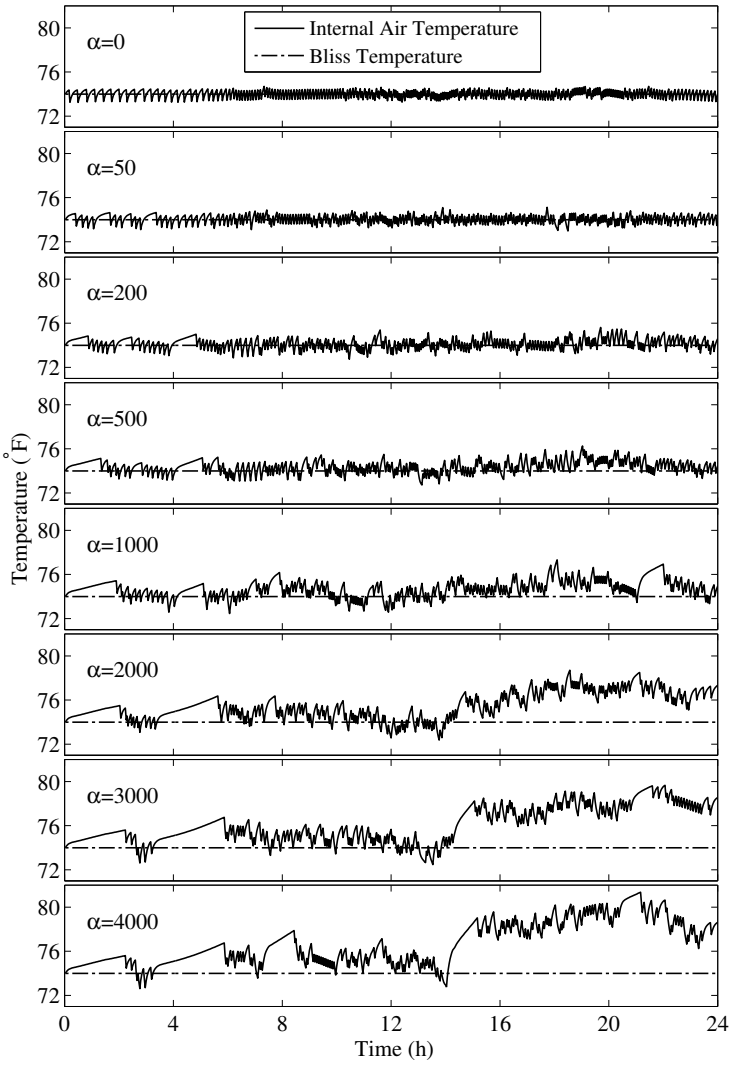

Figure 2.5 Variation of internal air temperature (T_n^a) with α.

makes a decision to switch off during the morning hours. For the extreme case of $\alpha = 0$, this switch occurs as soon as the resident leaves home. However, as α is increased, the A/C turns off earlier than that. It is also interesting to observe how the controller decides to cool down the house in anticipation of the resident's arrival at home at 5 p.m., and how this decision varies with different α values.

Table 2.2 summarizes the results, which follow a similar trend as for the previous experiment. Comparing Tables 2.1 and 2.2, we find that the cost of electricity and the energy consumption have decreased considerably. This is because the A/C is mostly turned off during the time R is

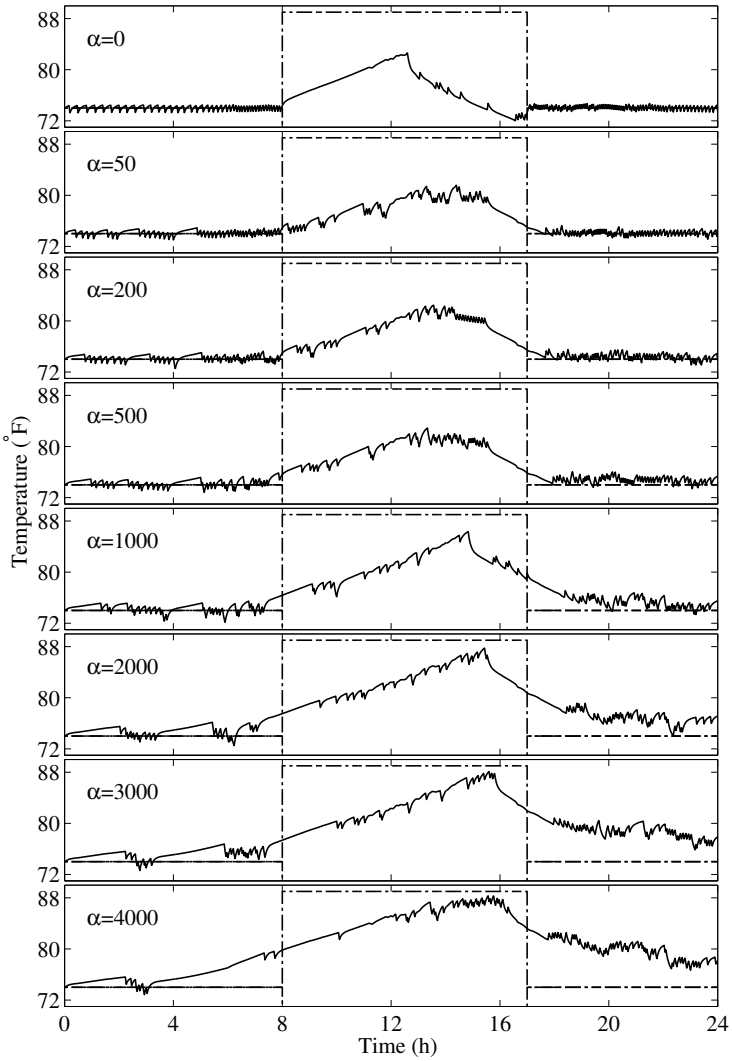

Figure 2.6 Variation of internal air temperature (T_n^a) with α and $k_{1n} = k_{2n} = 15$ °F while the resident is not at home.

not at home.

2.6 Conclusion

The purpose of this paper is to present the control of an A/C system by stochastic dynamic programming (SDP) to achieve optimal intertemporal trade-offs between thermal comfort and A/C energy costs for a household resident conditional on retail A/C energy prices and environmental conditions. A thermal comfort model is used to capture the thermal preferences of the resident.

Table 2.2 Results with Nonzero k_{1n}, k_{2n}

α	24-hour Electricity Cost ($)	24-hour Thermal Comfort (Utils)	24-hour Net Benefit (Utils)	24-hour Energy (kWh)
0	2.09	1075.2	1075.2	26.4
50	2.05	1073.1	970.8	25.8
200	2.02	1067.6	664.3	25.4
500	1.96	1055.9	73.6	24.7
1000	1.88	990.6	-891.6	23.7
2000	1.71	826.1	-2594.8	21.4
3000	1.60	582.8	-4214.3	20.1
4000	1.49	287.9	-5670.8	18.5

The critical parameter α appearing in the household resident's net benefit function (2.7) plays a key role in the determination of the resident's optimal comfort/cost trade-offs. As detailed in Appendix 2.7.2, α reflects an attribute of the household resident—namely, his marginal benefit of income—that depends on his preferences and on his opportunities for the purchase of alternative goods; α is not a "control variable." As seen in Section 2.5, we envision our A/C controller as having an α "knob" that each household resident can fine tune to match his own particular preferences and choice environment. In Section 2.5 we provide numerical examples to show how different settings for this alpha "knob" for different residents would affect the A/C energy usages resulting from the optimal on-off A/C control settings generated by the A/C controller, all else equal.

In a possible future smart-grid scenario, dynamically varying price signals can be communicated to households, thereby achieving active demand response. Our thermal comfort model can form a basis for studying the aggregation of price-sensitive demand emanating from a residential area, since A/C systems constitute a substantial component of residential energy consumption during the summer. The methodology can also be adopted by LSEs to forecast price-sensitive load from their retail customers. Furthermore, there is an interesting feedback loop connecting wholesale load to wholesale prices to retail prices to retail load and back up to wholesale load. In fact, this feedback loop is currently being explored by means of systematic simulation

studies [41].

As stressed in Section 2.2, our study is agnostic regarding the exact method by which the LSE servicing the A/C energy needs of retail consumers determines the A/C energy prices. Clearly, however, the ability to offer retail energy contracts under which the prices charged vary dynamically with changing conditions could open up strategic opportunities for profit-seeking LSEs. This important topic is part of our ongoing research.

The general discrete-time SDP problem set out in Section 2.2 for the household resident does not assume a finite domain either for the control actions u_n or for the state vectors $\mathbf{x}_n$. For practical application, however, finite discretizations are introduced in Section 2.3 for the control and state domains that render our SDP formulation equivalent to a finite-horizon discrete-time Markov Decision Process (MDP). In future studies it would be of interest to compare and contrast our SDP solution approach to approaches that have been introduced in the literature for the approximate solution of MDP problems.

It is also of great interest to design a similar controller for inverter-based systems, which are rapidly gaining market share worldwide, because they offer increased efficiency and energy savings (albeit with increased capital cost). However, this is not the case in the United States, where most residential A/C systems are still commonly based on simple on/off control. Therefore, one important advantage of our simple "bang-bang" proposed control is that it lends itself to the retrofitting of existing systems (at least in the USA) with minimal intervention required on the mechanical A/C components. Nevertheless, the general mathematical formulation outlined in Section 2.2 certainly permits the formulation of a continuous problem, which would be appropriate for an inverter-based A/C system. This is an important topic for future work.

The general formulation (2.6) for the household resident's thermal comfort function set out in Section 2.2 permits thermal comfort to depend on the initial and final state vectors during period n as well as directly on n. For concrete illustration, however, Section 2.4 uses a simplified thermal comfort function (2.26) that depends only on the initial and final air temperature of the resident's house for any period n as well as on period-specific lower and upper bounds for the resident's comfort function reflecting whether the resident is actually at home during period n. In future studies it would be of great interest to explore more carefully the implications of

alternative thermal comfort function specifications for the welfare of household residents and for system performance more generally. Moreover, it would be important to refine further the physical model of the A/C system, in order to study the impact of improved modeling on the optimization results.

Finally, in future work we intend to implement the proposed intelligent A/C system controller in practice, and to conduct experiments to test its performance. The current study provides the theoretical underpinnings for this experimental validation.

2.7 Appendix

2.7.1 Luenberger Observer to Estimate the Internal Mass Temperature

The ETP model (2.13)–(2.14) can be written as

$$\begin{bmatrix} \dot{T}^a \\ \dot{T}^m \end{bmatrix} = \begin{bmatrix} A_{11} & A_{12} \\ A_{21} & A_{22} \end{bmatrix} \begin{bmatrix} T^a \\ T^m \end{bmatrix} + \begin{bmatrix} \mathbf{b}_1^T \\ \mathbf{b}_2^T \end{bmatrix} \mathbf{w} \tag{2.28}$$

where A_{11}, A_{12}, A_{21} and A_{22} are the scalar elements of the matrix $\mathbf{A}$, and $\mathbf{b}_1^T$ and $\mathbf{b}_2^T$ are the two rows of the matrix $\mathbf{B}$. An estimate for the mass temperature can be constructed as

$$\dot{\hat{T}}^m = (A_{22} - \tilde{K}A_{12})\hat{T}^m + A_{21}T^a + \mathbf{b}_2^T\mathbf{w} + \tilde{K}(\dot{T}^a - A_{11}T^a - \mathbf{b}_1^T\mathbf{w})\,. \tag{2.29}$$

The gain $\tilde{K}$ is chosen such that $A_{22} - \tilde{K}A_{12} < 0$, in which case it can be shown that the error $T^m - \hat{T}^m$ asymptotically approaches zero as $t \to \infty$ [42]. However, this estimator requires knowledge of $\dot{T}^a$, which is unknown. To eliminate $\dot{T}^a$, we let $z \equiv \hat{T}^m - \tilde{K}T^a$, and (2.29) leads to a modified estimator in terms of z, given by

$$\dot{z} = (A_{22} - \tilde{K}A_{12})z + [(A_{22} - \tilde{K}A_{12})\tilde{K} + A_{21} - \tilde{K}A_{11}]T^a + (\mathbf{b}_2^T - \tilde{K}\mathbf{b}_1^T)\mathbf{w}\,. \tag{2.30}$$

The mass temperature is estimated from $\hat{T}^m = z + \tilde{K}T^a$. This observer logic could be readily programmed in the wall unit, in discrete-time form. For the simulation studies of Section 2.5, the gain was set to $\tilde{K} = -7$.

2.7.2 Extended Motivation for the Comfort/Cost Trade-off Model

Here we present additional motivation for the form of resident R's comfort/cost trade-off problem (2.10) set out in Section 2.2.1. In particular, we show that, for an appropriate choice of α, the solution of this problem can be viewed as a necessary condition for the solution of a more comprehensive problem involving the budget-constrained maximization of the benefit attained by R over periods $1, \ldots, N$ from the consumption of multiple goods in addition to thermal comfort.

As is standard in microeconomic treatments of multi-good optimization problems, suppose the multi-good benefit obtained by R over periods $1, \ldots, N$ is given by the function

$$W(\mathbf{u}, \mathbf{y}) = \sum_{n=1}^{N} \beta_n G(\mathbf{x}_n, S_n(\mathbf{x}_n, u_n, \boldsymbol{\nu}_n), n) + Z(\mathbf{y}) \,, \tag{2.31}$$

where the state vectors $\mathbf{x}_n$ satisfy the state equations (2.1) and (2.2), and the dependence of W on the exogenously given terms $\boldsymbol{\nu}$ and $\bar{\mathbf{x}}_1$ has been supressed from the notation. As in Section 2.2.1, the summation term measures the benefit (comfort) attained by R from the thermal conditions inside his house during periods $1, \ldots, N$. Now, however, there is also a second term, $Z(\mathbf{y})$, measuring the benefit (satisfaction) attained by R from the consumption of a vector $\mathbf{y} = [y_1, \ldots, y_m]^T$ of m additional types of goods during periods $1, \ldots, N$. Assume that R strictly prefers more of each of these goods to less, all else equal, implying that $Z(\mathbf{y})$ is a strictly increasing function of y_j for each $j = 1, \ldots, m$.

Let $\mathbf{p}^y = [p_1^y, \ldots, p_m^y]$, where p_j^y denotes the dollar amount paid by R per unit of consumption of good j. Also, assume that the A/C electric energy prices $\mathbf{p} = [p_1, \ldots, p_N]$, the goods prices $\mathbf{p}^y$, and the environmental conditions $\boldsymbol{\nu} = [\boldsymbol{\nu}_1, \ldots, \boldsymbol{\nu}_N]$ are known by R prior to the start of period 1. Let I (\$) denote R's target total income expenditure level for periods $1, \ldots, N$, and let $\mathbf{u} = [u_1, \ldots, u_N]$ and $\mathbf{y}$ denote the choice vectors for R.

Now consider the following optimization problem for R involving the maximization of his multi-good benefit function (2.31) subject to a budget constraint:[7]

$$\max W(\mathbf{u}, \mathbf{y}) \tag{2.32}$$

[7] For expositional simplicity, the restriction of u_n to some admissible domain U and the restriction of $\mathbf{y}$ to the nonnegative orthant in Euclidean m-space are ignored below. Also, the assumed nonsatiation of R with respect to consumption of $\mathbf{y}$ guarantees that R will satisfy his budget constraint as a strict equality.

with respect to choice of $\mathbf{u}$ and $\mathbf{y}$, subject to

$$\sum_{n=1}^{N} \beta_n C(p_n, \tilde{e}_n(u_n, \boldsymbol{\nu}_n)) + \mathbf{p}^y \cdot \mathbf{y} = I\,. \tag{2.33}$$

Let α denote the Lagrange multiplier corresponding to the budget constraint (2.33), and form the Lagrangian function $\mathcal{L}$ as follows:

$$\mathcal{L}(\mathbf{u}, \mathbf{y}, \alpha, I) = W(\mathbf{u}, \mathbf{y}) + \alpha \left[I - \sum_{n=1}^{N} \beta_n C(p_n, \tilde{e}_n(u_n, \boldsymbol{\nu}_n)) - \mathbf{p}^y \cdot \mathbf{y} \right] \tag{2.34}$$

Suppose the usual Karush-Kuhn-Tucker (KKT) first-order necessary conditions expressed in terms of the Lagrangian function $\mathcal{L}$ result in unique solutions $(\mathbf{u}^*, \mathbf{y}^*, \alpha^*)$ for $\mathbf{u}$, $\mathbf{y}$, and α. Let these solutions be expressed in the form

$$(\mathbf{u}^*, \mathbf{y}^*, \alpha^*) = (\mathbf{u}(I), \mathbf{y}(I), \alpha(I))\,, \tag{2.35}$$

where dependence on all exogenous variables except income I has been suppressed from the notation. Given certain regularity conditions, it follows by the envelope theorem[8] that $\alpha(I)$ measures R's marginal benefit of income[9] in the sense that

$$\alpha(I) = \frac{dW(\mathbf{u}(I), \mathbf{y}(I))}{dI}\,. \tag{2.36}$$

That is, $\alpha(I)$ measures the change in R's optimized multi-good benefits with respect to a change in his income I, evaluated at the solution point.

Finally, here is the interesting observation that motivates this appendix discussion. If α is pre-set at the level $\alpha(I)$ in the Lagrangian function $\mathcal{L}$ in (2.34), this function separates into two parts, one involving only $\mathbf{u}$ and the other involving only $\mathbf{y}$, as follows:

$$\sum_{n=1}^{N} \beta_n \left[G(\mathbf{x}_n, \mathbf{x}_{n+1}, n) - \alpha(I) C(p_n, \tilde{e}_n(u_n, \boldsymbol{\nu}_n)) \right] \tag{2.37}$$

and

$$Z(\mathbf{y}) + \alpha(I)[I - \mathbf{p}^y \cdot \mathbf{y}]\,. \tag{2.38}$$

[8] Applied to the problem at hand, the envelope theorem [43, Chap. 1, Thm. 1.F.1] guarantees that:

$$dW(\mathbf{u}(I), \mathbf{y}(I))/dI = d\mathcal{L}(\mathbf{u}(I), \mathbf{y}(I), \alpha(I), I)/dI = \partial\mathcal{L}(\mathbf{u}(I), \mathbf{y}(I), \alpha(I), I)/\partial I = \alpha(I)$$

where d denotes total differentiation and ∂ denotes partial differentiation.

[9] In the economics literature, in which consumer benefits are assumed to be measured by "utility functions," it is standard to refer to α as a marginal utility of income measure.

The optimal setting of $\alpha(I)$ in (2.37) and (2.38) guarantees that R's income I is optimally split between expenditures on electric energy for A/C and expenditures on the consumption goods $\mathbf{y}$. Consequently, the two parts can be separately treated as individual optimization problems.

In particular, the maximization of (2.37) with respect to $\mathbf{u}$, the approach taken in Section II, results in the satisfaction of the KKT necessary first-order conditions for the choice of $\mathbf{u}$ corresponding to the more comprehensive budget-constrained multi-good benefit maximization problem handled in this appendix that involves a simultaneous choice of both $\mathbf{u}$ and $\mathbf{y}$. Thus, by appropriate trial-and-error experimentation, resident R could arrive at a setting for the comfort/cost trade-off factor α in (2.7) that approximately achieves his optimal A/C energy usage solution for this more comprehensive problem.

CHAPTER 3. EFFECTS OF PRICE-RESPONSIVE RESIDENTIAL DEMAND ON RETAIL AND WHOLESALE POWER MARKET OPERATIONS

A paper published in the

Proceedings of the IEEE Power and Energy Society General Meeting,

San Diego, CA, July 22-26, 2012

Auswin George Thomas, Chengrui Cai, Dionysios C. Aliprantis, and Leigh Tesfatsion

Abstract

This paper describes a computational platform for studying the effects of price-responsive residential demand for air-conditioning (A/C) on integrated retail and wholesale power market operations. The physical operations of the A/C system are represented by means of the physics-based equivalent thermal parameter model. Residential A/C energy usage levels are determined by means of a stochastic dynamic-programming optimization in which the daily comfort attained by the resident is optimally traded off against his daily energy costs, conditional on retail energy prices, environmental conditions, and A/C operational constraints. An example is provided to illustrate the dynamic feedback loop connecting residential A/C load, the energy prices determined at wholesale conditional on A/C load, and the retail energy prices offered to residential A/C consumers by wholesale energy buyers.

3.1 Introduction

Traditionally in the United States the generation, transmission, and distribution of electric power was monopolistically controlled by vertically integrated utilities with retail load obli-

gations serviced under retail rates fixed by state and/or local agencies. As a result of the restructuring movement over the past fifteen years, however, over half of all generating units are now operating within ISO/RTO-managed energy regions in which generation is required to be unbundled from transmission operations. Moreover, under recent efforts to incorporate smart-grid features, the power industry is increasingly experimenting with means for permitting more active participation by retail consumers in power industry operations.

One advance along these lines has been the development of advanced metering infrastructure whose future implementations might be able to report dynamic price signals to retail consumers reflecting actual energy costs. These costs in general will be related to the charges paid at wholesale by load-serving entities (LSEs). This sets up an interesting feedback dynamic between retail and wholesale levels of operation: Retail loads enter into the determination of wholesale energy prices, which in turn affect the retail prices set by LSEs through retail dynamic-price contracts.

This paper describes a computational platform to investigate the effects on retail and wholesale power system operations when the air-conditioning (A/C) systems of household residents are responsive to price. Residential A/C constitutes a substantial component of load, especially during hot days. A critical requirement for this analysis is the representation of the load profiles arising at the wholesale level from price-responsive retail demands.

Several attempts have been made in the past to achieve a high-fidelity modeling of load. For example, Kosterev et al. [44] discuss the latest advances in load modeling for the study of power systems in the Western Electricity Coordinating Council (WECC) region. Also, Schneider and Fuller [45] provide a detailed discussion of end-use load modeling for distribution analysis. In particular, note that loads with thermal cycles can utilize thermal storage to shift loads to periods with lower prices. Heating, Ventilation, and Air-Conditioning (HVAC) systems constitute a major portion of the load having thermal cycles. The power consumption of an HVAC system is directly dependent on its set-point. Hence, a simple logic such as increasing (decreasing) the set-point of an HVAC system in the cooling mode during high (low) prices can be used to achieve a price-responsive HVAC controller. Schneider et al. [46] use the set-point adjustment method to study the effects of price-sensitive HVAC demand on the operations of a

distribution feeder, where retail prices are exogenous values set by the modelers. Zhou et al. [47] extend these studies by using real-time price realizations to test the effects of price-sensitive HVAC demand, whereas Fuller et al. [48] use a price realization from a double-auction capacity management market.

Although the simple set-point adjustment method considered in these earlier studies permits the straightforward derivation of a price-sensitive load profile across residents, it does not take into account in any carefully considered manner the preferred comfort-cost trade-offs of each resident. Moreover, the dynamic circular flow connecting retail loads, wholesale energy prices, and retail energy prices is not fully modeled.

Building on prior work by the authors and their collaborators [49], this study utilizes a computational model of a household with an intelligent A/C system that responds not only to price signals but also to the household resident's preferred comfort-cost tradeoffs. The physical operations of the A/C system are represented by means of the physics-based Equivalent Thermal Parameter (ETP) model [34, 35]. The resident's A/C energy usages are then determined by means of a stochastic dynamic-programming optimization in which the daily comfort attained by the resident is optimally traded off against his daily energy costs. This optimization is conditional on resident attributes (e.g., preferences), structural attributes (e.g., house insulation), environmental attributes (e.g., outside temperature), A/C operational attributes, and retail energy prices.

Given this formulation for a single household, a collection of households is then computationally modeled, each with an intelligent A/C system but with differing residential preferences and structural attributes. The price-sensitive retail loads arising from this diverse collection of households affect the determination of wholesale energy prices and hence the costs paid by LSEs for their wholesale energy purchases. These LSE costs in turn affect the retail energy prices that the LSEs charge their retail household customers. The overall effects of this feedback loop on system performance are then studied by means of controlled computational experiments.

The remainder of this paper is organized as follows. Section 3.2 describes the computational platform. Section 3.3 presents a five-bus test case, and Section 3.4 explains the methodology used to represent aggregate retail load at any load bus by means of distribution feeder data.

The general simulation methodology used to implement an integrated modeling of retail and wholesale power system operations with price-responsive A/C residential demands is presented in Section 3.5 and illustrated for the five bus test case in Section 3.6. Concluding remarks are given in Section 3.7.

3.2 Integrated Retail and Wholesale Test Bed

This study makes use of an agent-based platform to model retail and wholesale power markets operating over transmission and distribution networks. This platform, referred to as the Integrated Retail and Wholesale (IRW) Power System Test Bed [50], makes use of an extended version[1] of AMES [51] to simulate a wholesale power market adhering to standard market practices, and GridLAB-D to model end-use loads.

This extended version of AMES (*A*gent-based *M*odeling of *E*lectrical *S*ystems) is a modular agent-based computational platform for the study of wholesale power systems that has been developed in Java by a group of researchers at Iowa State University. It is based on the actual design of U.S. restructured wholesale power markets adhering to standards set by the U.S. Federal Energy Regulatory Commission. The agents in AMES include an Independent System Operator (ISO), Generating Companies (GenCos), and Load Serving Entities (LSEs). The GenCos and the LSEs participate in a two-settlement system consisting of a day-ahead and a real-time market operated and settled by the ISO. Transmission grid congestion is managed by Locational Marginal Prices (LMPs).

GridLAB-D [52] is a modular agent-based energy distribution platform developed by DOE researchers at Pacific Northwest National Laboratory (PNNL) that provides detailed models of loads arising from residential, industrial and commercial retail consumers with a variety of appliances and equipment. The MySQL database server is used to facilitate data storage for analysis and data transfer between the various applications. As will be clarified in later sections, GridLAB-D is used in this study to generate the non-price-responsive load profiles for modeled

[1] The released AMES version (V2.05) does not consider discrepancies between cleared loads in the day-ahead market and actual real-time loads. The extended version of AMES has a fully operating two-settlement system (day-ahead and real-time markets operating in tandem) that prices such load discrepancies at real-time market prices, as is standard practice in US restructured electric energy regions.

households.

3.3 Five-Bus Test Case

For concrete illustration, consider a 5-bus test case with five GenCos, three LSEs, and a high-voltage transmission grid consisting of six lines, as shown in Fig. 3.1.[2] The power flow limit (250 MW) on the line between buses 1 and 2 typically results in congestion occurring on this line throughout the day.

As explained more carefully in Section 3.4, the demand at bus 4 (where LSE 3 is located) is extracted from a realistic representation of a distribution system using a GridLAB-D distribution feeder. Demand at all other load buses is modeled by means of the exogenously specified load profiles shown in Fig. 3.2(c), which have a coincident peak observed at hour 18.

The peak power of the load at buses 2 and 3 is on the order of several hundred MW. On the other hand, the power rating for the distribution feeders modeled in GridLAB-D ranges from 948 KVA to 17 MVA depending on the type of load area (e.g., rural, suburban, heavy urban) and the composition of the load (residential, agricultural, and industrial)[53]. To obtain a load at bus 4 of approximately the same magnitude, the GridLAB-D loads are simply scaled by an appropriate factor.

The marginal cost function for GenCo i is given by

$$\frac{dC(P_{Gi})}{dP_{Gi}} = a_i + 2b_i P_{Gi},\ Cap_i^L \leq P_{Gi} \leq Cap_i^U \tag{3.1}$$

for $i = 1, 2, \ldots, 5$. The specific parameter values used in this study for the GenCos' marginal cost functions and their lower/upper generation capacity limits are listed in Table 3.1.

3.4 Load aggregation

A "heavy urban" distribution feeder is selected as the distribution feeder from GridLAB-D to model aggregate load at bus 4 of the 5-bus test case. This distribution feeder, labeled as R1-12.47-4 in the taxonomy feeder model [54], represents a heavily populated suburban area

[2] Apart from the modeling of price-responsive load for LSE 3, explained below, complete input data for the 5-bus test case used in this study are provided in the input data file for the 5-bus test case (with 100% fixed loads) included in the data directory of the AMES(V2.05) download package [51].

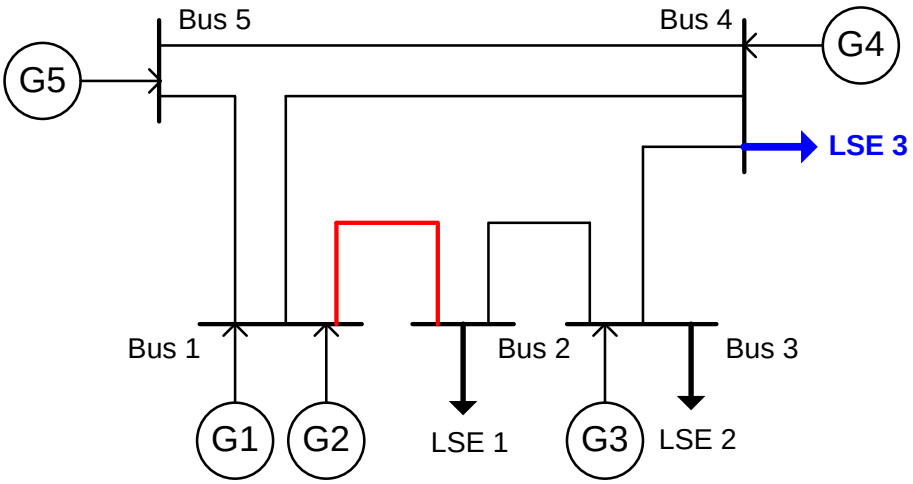

Figure 3.1 Power grid for the 5-bus test case.

Table 3.1 Parameter values for the GenCos' marginal cost functions and lower and upper generation capacity limits.

GenCo	a $/(MW)	b $/(MW^2)	Cap^L MW	Cap^U MW
1	14	0.005	0	110
2	15	0.006	0	100
3	23	0.010	0	520
4	30	0.012	0	200
5	10	0.007	0	600

mainly composed of single-family houses and heavy commercial loads. There are 38 residential and 12 commercial transformers installed in this feeder, and the peak load is 5.3 MW.

The feeder contains hundreds of houses with detailed end-use loads, such as traditional A/C systems, lights, and various types of appliances. For the purposes of this study, the traditional A/C systems are replaced with intelligently controlled A/C systems as modeled in [49]. The feeder load is thus divided into two parts: non price-responsive load obtained by simulating the feeder with all A/C systems in all households turned off; and the intelligently controlled A/C load, which is calculated separately. The non price-responsive load can be simulated off-line in

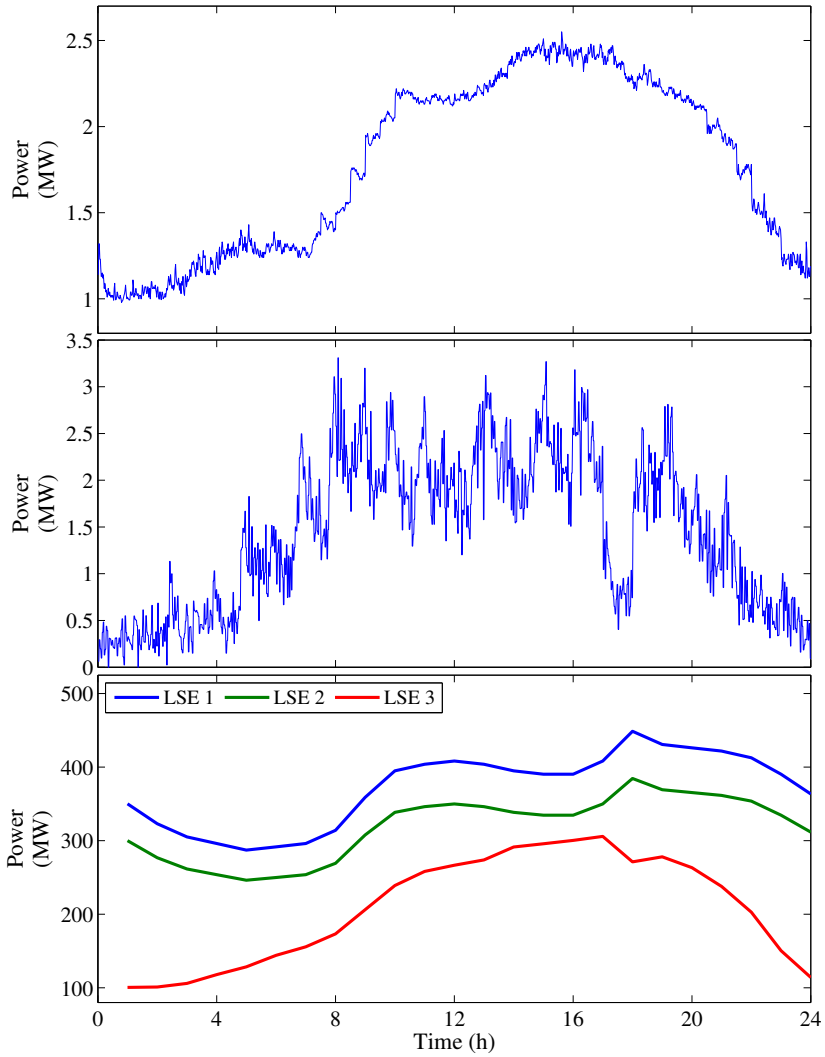

Figure 3.2 a) Non-price-responsive load in the distribution feeder; b) Intelligent A/C load in the distribution feeder; c) Daily load profiles for the LSEs, averaged by hour.

GridLAB-D for the duration of the simulation. This eliminates the need to run GridLAB-D in tandem with AMES. For simplicity, the same load profile is used for each day of the simulation, as shown in Fig. 3.2(a). This is scaled up to 220 MW peak in order to match the power rating of other buses in AMES.

The distribution feeder comprises 652 households, and a real power system may feed tens of thousands of households in each bus. If the distinct structural attributes (e.g., insulation levels and size dimensions) of each household were to be modeled, the simulation would become computationally intractable. Consequently, the households are divided into ten groups (of 65

households), where each house within a particular group has identical structural attributes.

The thermal dynamics of each house are modeled using the ETP model [34, 35]. More precisely, the ETP model supposes that the dynamics of the inside air temperature T^a and the inside mass temperature T^m at time t are defined by a system of two first-order linear differential equations:

$$\frac{dT^a}{dt} = \frac{1}{C^a}\left[(T^o - T^a)U^a + (T^m - T^a)U^m + \dot{Q} + \dot{Q}^a\right] \tag{3.2}$$

$$\frac{dT^m}{dt} = \frac{1}{C^m}\left[(T^a - T^m)U^m + \dot{Q}^m\right], \tag{3.3}$$

where

$$\dot{Q}^a = f(\dot{Q}^s, \dot{Q}^i) \tag{3.4}$$

$$\dot{Q}^m = g(\dot{Q}^s, \dot{Q}^i). \tag{3.5}$$

In these equations, C^a is the heat capacity (BTU/°F) of the internal air mass, C^m is the heat capacity (BTU/°F) of the internal solid mass, U^a is the thermal conductance (BTU/h/°F) between internal and external air mass defining the thermal envelope of the house and U^m is the thermal conductance (BTU/h/°F) between the internal air mass and the solid mass. T^o is the outside temperature (°F). $\dot{Q}^s$ is the heat flow rate (BTU/h) from the solar radiation, and $\dot{Q}^i$ is the heat flow rate (BTU/h) from internal appliances and occupants.

The term $\dot{Q}$ that appears in (3.2) is the heat flow rate (BTU/h) from the A/C system to the internal air mass. It is dependent on the A/C rating (BTU/h) and the latent cooling load (i.e., the unwanted moisture that needs to be removed) which depends on the relative humidity. The overall electricity power consumption depends on $\dot{Q}$ and the coefficient of performance COP (unit-free) of the A/C. The structural attributes of the ten groups of households along with their operational attributes are listed in Table 3.2.

The 65 household residents within each particular group are then allowed to have different A/C comfort-cost trade-off preferences as captured by a "marginal utility of income" parameter α [49] varying over eight different possible settings. For simplicity, the residents' temperature "bliss points" are assumed equal. In total, then, the distribution feeder includes $10 \times 8 = 80$

Table 3.2 Structural and operational attributes of the ten groups of households

Group	C^a	C^m	U^a	U^m	COP	A/C Rating
1	600	4791	180	6167	3.4	30000
2	1283	10348	432	10473	3.1	72000
3	1477	8745	517	11592	3.4	78000
4	414	2724	235	4812	2.5	30000
5	982	5398	439	8663	3.0	72000
6	1113	8542	506	9465	3.3	78000
7	1036	8745	601	8997	2.7	84000
8	710	5046	497	6921	2.7	66000
9	419	2267	542	6617	2.3	78000
10	1236	6662	924	10089	2.7	114000

distinct household types differing by structural and/or preference parameter settings. This approach results in a tractable modeling for diverse price-sensitive A/C residential demands.

Fig. 3.2(b) depicts the aggregated intelligent A/C load of the distribution feeder for an arbitrary day, conditional on environmental conditions and on retail price, shown in Figs. 3.3 and 3.4, respectively. Day-ahead forecasts of the environmental conditions are used for scheduling, while the real-time conditions are used to generate the actual load of the intelligent A/C system. The decrease in the intelligent A/C load at hour 18 (see Fig. 3.2(b)) is due to the peak retail price observed at that hour (based on the demand bids submitted by the LSEs the previous day), which is shown in Fig. 3.4. The peak power from the intelligent A/C loads is scaled up to 50 MW. This power level for the price-responsive demand constitutes around 20% of the total feeder load. The peak load of the distribution feeder is around 5 MW, which is less than the rating of the feeder (5.3 MW). Fig. 3.2(c) depicts the total aggregated load at the wholesale level at bus 4 (where LSE 3 is located), averaged over an hour in accordance with standard market practices.

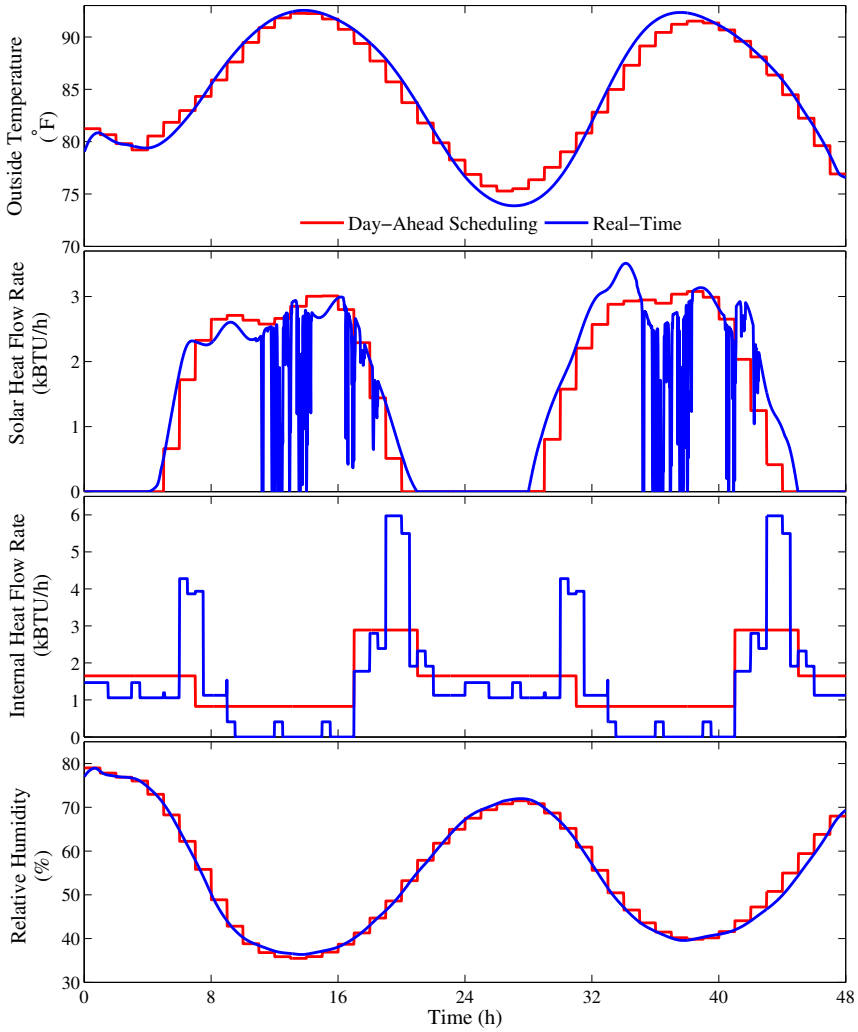

Figure 3.3 Variation of environmental parameters for day-ahead scheduling and real-time simulation.

3.5 Simulation Methodology

The logical flow of a simulation run is depicted in Fig. 3.5. Each simulation run can be decomposed into two parts, off-line and on-line. The off-line part involves initial configuring for the distribution feeder(s) and for AMES.[3] The on-line part schematically depicts the dynamic operation of the AMES two-settlement system (parallel day-ahead and real-time market

[3]Although in this study the load at only one AMES bus is extracted from the retail power system, the simulation methodology presented in this section assumes a more general case in which multiple AMES buses are potentially extended with loads extracted from retail power systems.

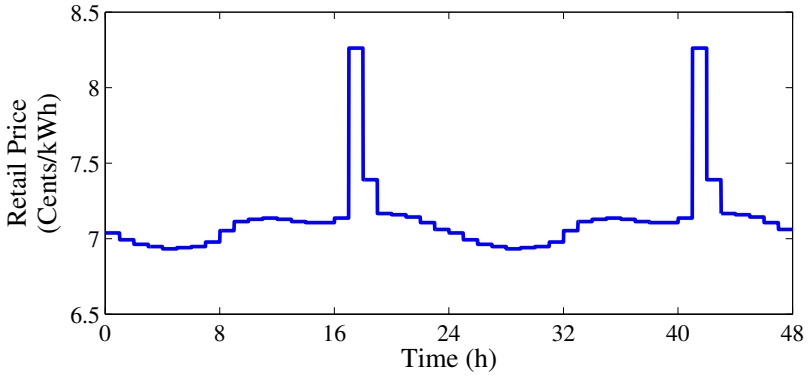

Figure 3.4 Retail price variation.

clearing).[4]

In the off-line part, the distribution feeder is first selected, and then the structural house parameters required for implementation of the ETP model are then extracted. Next, to obtain a daily non price-responsive load profile at each feeder-extended AMES bus, a simulation is performed on each feeder with all conventional A/C systems turned off for all houses.

As an additional off-line step, AMES has to be initialized on the initial simulation day 1 with "cleared" LSE demand bids for day 2 (i.e., an amount of energy scheduled to be purchased by each LSE for each hour of day 2), together with 24 hourly energy prices (LMPs) for day 2. These LMPs are interpreted as the (forward) market clearing price solutions determined in the day-ahead market on day 1 (along with cleared energy bid/offer solutions) for each hour of the following day. These LMPs also determine the costs paid by LSEs on day 1 for their cleared demand bids for day 2. The 24 hourly retail energy prices that the LSEs charge to their residential customers during day 2 are determined as a function of these day-1 costs. For example, if an LSE on day 1 pays p \$/kWh for its cleared demand bid for noon on day 2, it might set its retail energy price for noon on day 2 equal to p plus some mark-up amount m to cover billing and other services.

In the on-line part, a Data Management Program (DMP) retrieves from AMES the 24 hourly retail energy prices determined for day 2, using an SQL database server, and passes

[4] A two-settlement system design for wholesale power system operations has now been adopted in each of the seven U.S. ISO/RTO-managed energy regions: namely, CAISO, ERCOT, ISO-NE, MISO, NYISO, PJM, and SPP.

these retail energy prices to the intelligent A/C system for each house. Each of these intelligent A/C systems then calculates the actual A/C loads for day 2 given these retail energy prices, conditional on its own particular house and resident parameters, home appliance schedule, and the environmental conditions throughout the day.

The DMP then superimposes the total A/C load at each feeder-extended bus with the total non price-responsive load at each feeder-extended bus to form an actual hourly total load (for simplicity, the real-time market is run on an hourly basis in this study) for day 2. These loads are then appropriately scaled up to form the aggregate hourly total load for day 2 at each feeder-extended bus, and passed back to AMES via the SQL database server.

Once AMES receives the aggregate hourly total load for day 2 at each feeder-extended bus along with the loads at all other buses, it can run and clear the real-time market for day 2. This results in real-time LMPs that are used to price any discrepancies between the LSE demand bids for day 2 (contracted in the day-ahead market on day 1) and the realized loads arising from actual household energy usage on day 2.

In parallel with these real-time market operations on day 2, the profit-seeking AMES LSEs submit demand bids into the AMES day-ahead market on the morning of day 2 based on forecasted retail loads for day 3, taking into account the net earnings they obtained from both day-ahead and real-time settlements as a result of their past demand bids.[5] The AMES ISO then clears the day-ahead market on day 2, resulting in 24 hourly energy prices (LMPs) and 24 hourly energy dispatch levels scheduled for the next day 3. These LMPs determine the costs paid by LSEs on day 2 for their cleared hourly energy demand bids for day 3. The 24 hourly retail energy prices that the LSEs charge to their residential customers during day 3 are determined as a function of these day-2 costs.

This sequence of steps is then repeated until a user-specified terminal day.

[5] AMES permits any decision-making agent to have reinforcement learning capabilities. In general, the profit-seeking AMES LSEs have two learning tasks: namely, to update their daily load forecasts, and to update their daily demand bids based on all relevant past observed data and possibly, also, on strategic trading considerations.

3.6 Illustrative Example

In this section the 5-bus test case described in Section 3.3 is used to illustrate the simulation methodology outlined in Section 3.5. Recall that LSEs 1 and 2 located at buses 2 and 3 service fixed load profiles each day. In contrast, LSE 3 at bus 4 services the energy requirements of retail customers whose energy usages are a mixture of non-price-responsive load and intelligent load arising from smart A/C systems.

The 5-bus test case simulation begins on the morning of day 1 with the submission by LSE 3 at bus 4 of an initial demand bid to the ISO for use in the day-ahead market for day 2. This initial demand bid consists of a forecasted 24-hour load profile similar in shape to the 24-hour load profiles submitted as demand bids to the ISO on the morning of day 1 by LSE 1 and LSE 2; see Fig. 3.2(c). Also on the morning of day 1, the five GenCos submit supply offers[6] to the ISO for use in the day-ahead market on day 2 that consist of their true marginal cost functions and their true capacity limits; see Table 3.1.

The day-ahead market on day 1 is then cleared by the ISO during the afternoon of day 1 using a standard DC optimal power flow formulation, and the resulting hourly day-ahead market LMPs ($/MWh) and dispatch levels (MW) are posted in the evening of day 1. The LSE 3 passes the day-ahead LMPs for bus 4 to its retail customers, amplified by a mark-up factor m = $50/MWh. The actual hourly loads at bus 4 on day 2 are then determined as explained in Section 3.5.

A new day-ahead market opens on the morning of day 2. Since actual load data have not yet been observed, the demand bids submitted by all three LSEs for this day-ahead market on day 2 are unchanged from day 1. Day-ahead market activities for day 2 then proceed as for day 1. Actual hourly loads are also now realized in the real-time market on day 2.

By the morning of day 3, however, LSE 3 has access to the realized load data for day 2 and can use these data in an attempt to improve its demand bid (load profile forecast) for day 3. For this illustrative example, the following simple forecast methodology is adopted for

[6] To simplify the illustration, the demand bids (load profiles) submitted by LSE 1 and LSE 2 on day 1, and the supply offers submitted by the five GenCos on day 1, are repeated as their daily demand bids and supply offers throughout the simulation.

Table 3.3 Simulation results for bus 4 at the peak-load hour 18

Day	Load^{DA} (MW)	Load^{RT} (MW)	ΔLoad (MW)	LMP^{DA} ($/MWh)	LMP^{RT} ($/MWh)	ΔLMP ($/MWh)	Net Earnings ($)
1	320.44	N/A	N/A	32.61	N/A	N/A	N/A
2	320.44	237.77	82.67	32.61	30.70	1.91	11730.30
3	237.77	234.06	86.38	30.70	30.61	2.00	11530.42
4	234.06	256.01	-18.24	30.61	31.12	-0.42	12793.03
5	256.01	280.90	-46.84	31.12	31.70	-1.08	13994.32
6	280.90	280.47	-24.45	31.70	31.69	-0.57	14009.48
7	280.47	271.07	9.83	31.69	31.47	0.23	13551.44

LSE 3: namely, starting on day 3, the load profile forecast that LSE 3 submits as its demand bid for the day-ahead market is the actual load profile observed for its retail customers on the previous day. Thus, LSE 3 submits a load profile each day that consists of hourly quantities with no explicit dependence on price or environmental conditions; yet these load profiles in fact arise in part from intelligent A/C systems responsive to both price and environmental conditions, hence they vary systematically over time in response to changes in these conditions. On each subsequent simulated day, the LSEs, GenCos, and ISO then proceed through the same progression of activities as on day 3.

Let the demand bid (forecasted load) submitted by LSE 3 in the day-ahead market on day D-1 for bus 4 at hour H on day D be denoted by $\text{Load}^{\text{DA}}_{H,D-1}$, and let the actual aggregate load realized in the real-time market for bus 4 at hour H on day D be denoted by $\text{Load}^{\text{RT}}_{H,D}$. Similarly, let the day-ahead LMP determined on day D-1 for bus 4 at hour H on day D be denoted by $\text{LMP}^{\text{DA}}_{H,D-1}$, and let the real-time LMP determined on day D for bus 4 at hour H on day D be denoted by $\text{LMP}^{\text{RT}}_{H,D}$. The *load forecast error* for bus 4 at hour H on day D is then calculated as

$$\Delta\text{Load}_{H,D} = \text{Load}^{\text{DA}}_{H,D-1} - \text{Load}^{\text{RT}}_{H,D}\,. \tag{3.6}$$

Similarly, the *price deviation* for bus 4 at hour H on day D is calculated as

$$\Delta\text{LMP}_{H,D} = \text{LMP}^{\text{DA}}_{H,D-1} - \text{LMP}^{\text{RT}}_{H,D}\,. \tag{3.7}$$

Key results for each of the first seven simulated days are reported in Table 3.3 for bus 4 at the peak-load hour 18. For clarity, the subtracted terms used to calculate the load forecast errors (3.6) and price deviations (3.7) are highlighted using the same color. As explained above, the LSE demand bids and GenCo supply offers for day 1 are the same as for day 2, hence the day-ahead LMPs for day 1 are the same as for day 2.

Ignoring the first two days used to initialize the simulation, the price deviations (3.7) are plotted in Fig. 3.6(a) for D varying from 3 to 7. Since all parameter values remain constant throughout the simulation, along with the daily demand bids of LSEs 1 and 2 and the daily supply offers of the five GenCos, these price deviations are entirely due to LSE 3's load forecast errors. These load forecast errors, in turn, arise due to randomly varying environmental conditions.

The net earnings of LSE 3 at bus 4 for any hour H of any simulated day D = 2,...,7 are determined as follows:

$$\begin{aligned}\text{NetEarnings}(H,D) = [m + \text{LMP}^{\text{DA}}_{H,D-1}] \cdot \text{Load}^{\text{RT}}_{H,D} - \text{LMP}^{\text{DA}}_{H,D-1} \cdot \text{Load}^{\text{DA}}_{H,D-1} \\ + \text{LMP}^{\text{RT}}_{H,D} \cdot [\text{Load}^{\text{DA}}_{H,D-1} - \text{Load}^{\text{RT}}_{H,D}]\,, \quad (3.8)\end{aligned}$$

where m denotes the mark-up added by LSE 3 to the day-ahead LMP. Collecting terms, (3.8) can equivalently be expressed as

$$\text{NetEarnings}(H,D) = m \cdot \text{Load}^{\text{RT}}_{H,D} + [\text{LMP}^{\text{DA}}_{H,D-1} - \text{LMP}^{\text{RT}}_{H,D}] \cdot [\text{Load}^{\text{RT}}_{H,D} - \text{Load}^{\text{DA}}_{H,D-1}]\,, \quad (3.9)$$

or, in more compact form, as

$$\text{NetEarnings}(H,D) = m \cdot \text{Load}^{\text{RT}}_{H,D} - \Delta\text{LMP}_{H,D} \cdot \Delta\text{Load}_{H,D}\,. \quad (3.10)$$

All else equal, $\text{LMP}^{\text{RT}}_{H,D}$ will tend to move in the same direction as $\text{Load}^{\text{RT}}_{H,D}$. This follows because the real-time aggregate supply curve for hour H of day D is upward sloping, and an increase in $\text{Load}^{\text{RT}}_{H,D}$ results in a rightward shift in the (vertical) real-time aggregate demand curve for hour H of day D. The second term on the right-hand-side of the equality in (3.9) will thus tend to be negative unless LSE 3's day-ahead hourly load forecast, $\text{Load}^{DA}_{H,D-1}$, is a perfect forecast of its real-time hourly aggregate load, $\text{Load}^{RT}_{H,D}$. Indeed, this is a deliberate

design feature of the two-settlement system to encourage accurate LSE load forecasting. Notice, however, that LSE 3 can still earn a positive profit if it is able to set the mark-up m sufficiently high.

The aggregate load profile at bus 4 for each of the simulated days 2 through 7 is shown in Fig. 3.6(b). LSE 3's corresponding hourly net earnings (3.10) are plotted in Fig. 3.6(c). Comparing Fig. 3.6(b) with Fig. 3.6(c), it is seen that LSE 3's hourly net earnings are strongly positively correlated with hourly real-time aggregate loads. The explanation for this correlation is that, for the simulation at hand, the load forecast errors (3.6) and price deviations (3.7) are very small compared to LSE 3's mark-up earnings $m \cdot [\text{Load}^{\text{RT}}_{H,D}]$ in (3.10). Hence, LSE 3's net earnings for each hour of day D are approximately determined by its mark-up earnings for this hour.

3.7 Conclusion

Given the increased penetration of price-responsive demand envisioned under smart grid initiatives, it is critically important to investigate the effects of this penetration on system operations at both retail and wholesale levels. Price-responsive retail energy demand affects wholesale load and hence wholesale energy prices, which in turn affect the energy prices set by wholesale energy buyers for their retail energy customers.

The primary purpose of the present study is to demonstrate, through concrete illustration, that computational platforms can be developed that permit the systematic study of integrated retail and wholesale power system operations with price-responsive demand. The platform reported in this study is still in a preliminary stage of development, and many possible improvements are under investigation.

For example, one major improvement would be to decrease the computation time needed to simulate the retail-wholesale feedbacks arising from price-responsive retail demand. A resort to parallel computing or supercomputing could speed up the process. The aggregation of the load is also at a very crude modeling stage. The simultaneous simulation of multiple distribution feeders would eliminate the need to scale up the retail load and would permit temporal and spatial load diversity to be captured with greater empirical verisimilitude. In addition, appropriate load

forecasting methods for LSEs servicing price-responsive retail demand need to be investigated. The ability of LSEs to use mark-ups over wholesale energy prices also needs to be more carefully examined. Higher mark-ups could lead to higher net earnings in the short-run, but could also ultimately result in lower net earnings if retail customers are able to vote with their feet to patronize lower-priced rival retailers. These and other important issues are subjects of ongoing and future research.

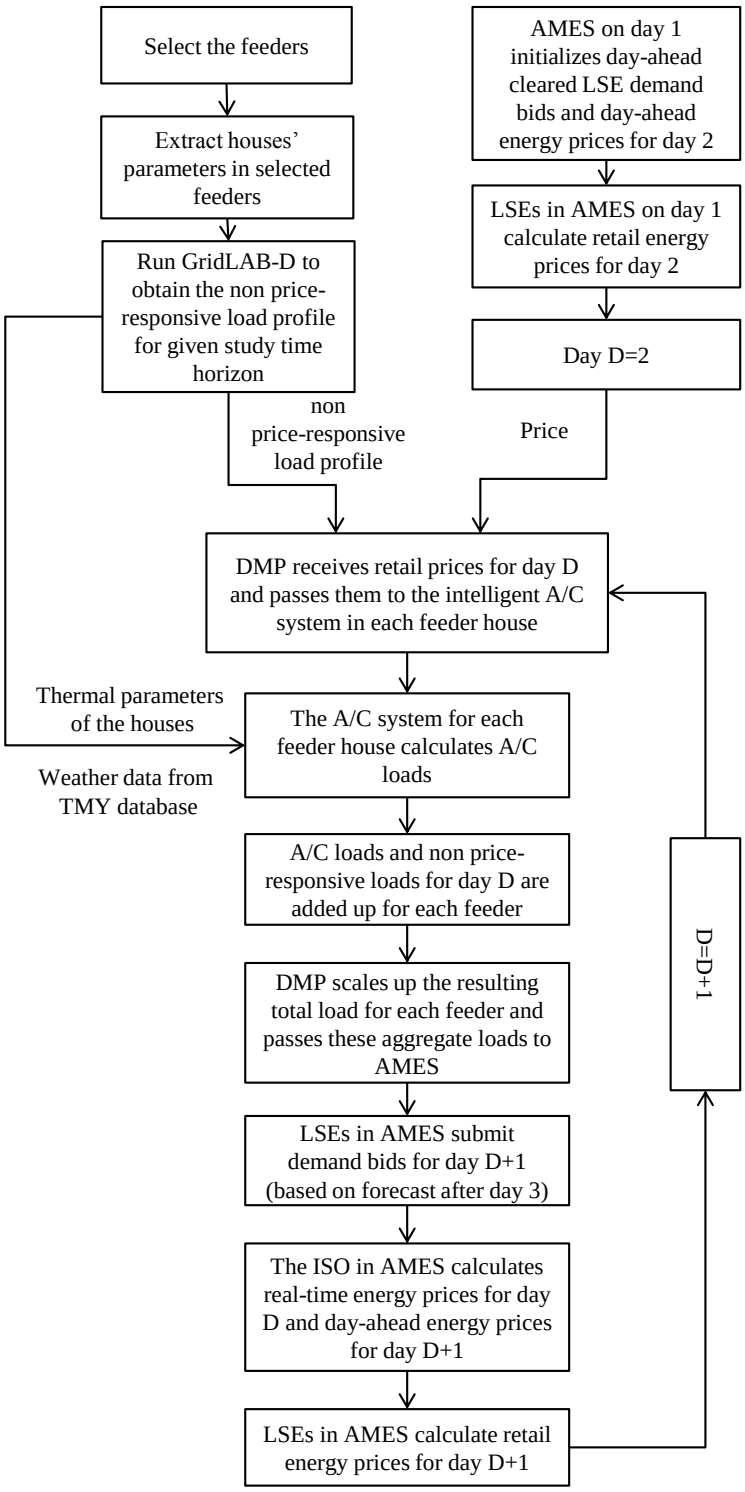

Figure 3.5 Flow diagram for a simulation run.

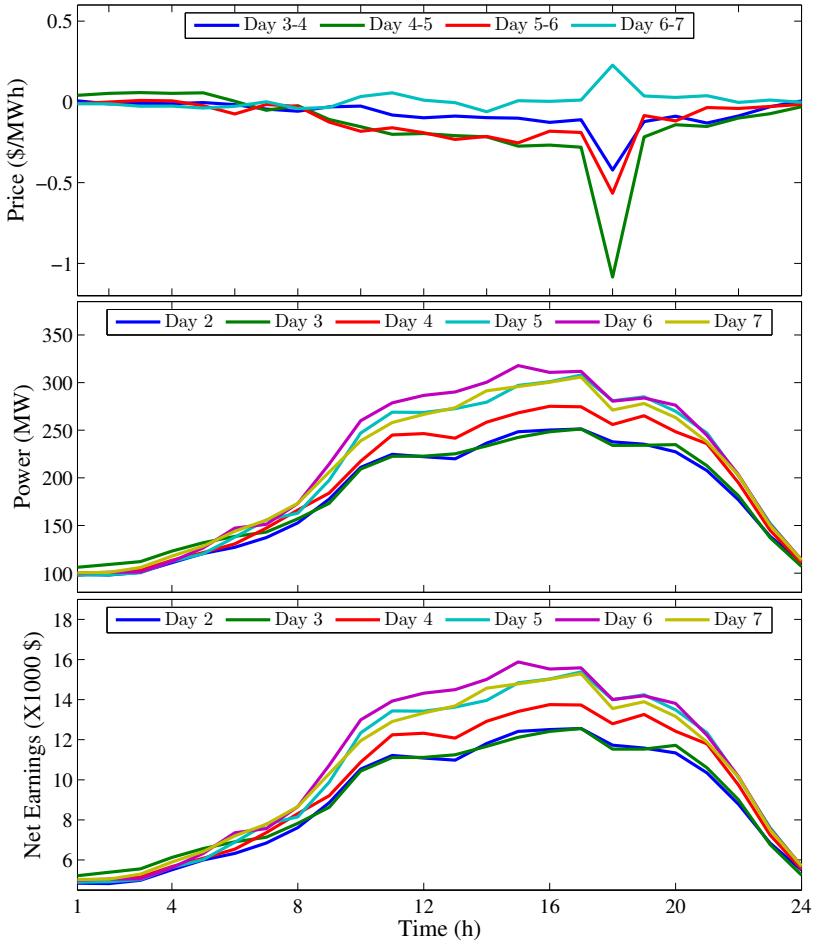

Figure 3.6 a) Differences between day-ahead and real-time LMPs; b) The aggregated load profile at bus 4; c) Hourly net earnings of LSE 3 from the two-settlement system.

CHAPTER 4. GENERAL CONCLUSION

The main motivation of this thesis is to demonstrate the use of residential air-conditioning systems to provide comfort and cost trade-offs to the resident and also provide indirect load control to the system. The peak load reduction achieved in the system results in the use of less expensive generation. Apart from the reduction of the peak load, the indirect load control methodology has other advantages. It facilitates the contribution of retail consumers to provide services to the power system. The active interaction of consumers (and thereby retail load) is one of the key aspects of the smart grid. It also demands the utilities to improve their efficiency in managing their customers as increased consumer participation would result in competition between different utilities. The utilities will have to perform to their best to attract retail consumers which would result in the overall reduction of the price signal and also improve the energy efficiency in the power system.

4.1 Contributions of the Thesis

One of the specific contributions of this thesis is the development of the intelligent A/C controller for residential households to provide comfort and cost trade-offs to the resident and to achieve indirect load control in the system. The thermal comfort of the resident is taken into account carefully and optimal intertemporal trade-offs between itself and the A/C energy costs for the resident is achieved. It is to be mentioned that these optimal trade-offs are conditional on resident's behavioral attirbutes, structural attributes of the house, retail energy price and environmental conditions.

The intelligent A/C controller can form the basis to study price-responsive demand in the distribution system. Several implementations of the A/C controller in a large distribution feeder

could be used by the utilities to study the behaviour of the consumers in response to various control signals whose preferences have been captured as accurately as possible from the electrical system's point of view.

Another contribution of the thesis is the development of the software framework necessary to integrate the retail and the wholesale system. This computational framework includes the price-responsive residential A/C demand that affects the price in the wholesale power market. The feedback loop is established as a result of the framework. Herein, the wholesale price is fed to the downstream consumers with the intelligent A/C controller. This generates a price-responsive demand that is fed back to the wholesale system that results in the generation of a new price signal corresponding to this load. This process continues in the form of a staggered feedback loop and preliminary results are reported based on this complex interactive feedback loop.

4.2 Possible Directions of Future Research

This thesis is just a preliminary investigation of the wide range of possibilites that exist. The following items are proposed as possible future research directions.

- Extension of the indirect load control methodology:

  As mentioned in Chapter 1, demand side management (DSM) has two types of load control: direct and indirect load control. Direct load control is equally beneficial to the system in several other aspects. Regulation services and load following require quick response from the load which is possible through direct load control. In indirect control, the consumers may or may not affect the retail load to a large extent depending on their preferences. Hence, a top-down approach which is achieved by direct load control could be analyzed. The effects of the retail load arising from direct load control on the wholesale and retail system will also have to be studied.

- Extension of the algorithm to other appliances:

  The A/C system is not the only system that has the potential to engage in active response. There are numerous appliances in a household such as dishwasher, refrigerator,

clotheswasher and water heater that also have the capability to be intelligent. Hence, the intelligent control algorithm can be implemented in other devices and a home management system can be formed.

- Improve the efficiency of the computational framework:

  The computational time needed to test the feedback effects arising from price-responsive retail demand has to be reduced as much as possible to run interesting experiments. A resort to parallel computing or supercomputing could speed up the process. This aspect forms an interesting future direction that gives much more ability to simulate the system at a more accurate level.

- Improvement in the feedback loop:

  The feedback loop is still at the preliminary level. Detailed representations of the distribution feeders are necessary to achieve realism in the results. Especially, multiple distribution feeders are important in aggregating the retail load. The utilities have to be careful in forecasting the load in the wholesale system as this forecast essentially determines how much the actual load deviates from the forecast. As the deviation between the forecast and the actual load usually results in a penalty, it gives the utilities great incentives to accurately forecast the retail load.

BIBLIOGRAPHY

[1] U.S. Department of Energy, "The Smart Grid: An introduction," Washington, DC, Sep. 2008. [Online]. Available: http://energy.gov/oe/downloads/smart-grid-introduction-0

[2] An Interdisciplinary MIT Study, "The future of the electic grid," Massachusetts Institute of Technology, Tech. Rep., 2011.

[3] Office of Electricity Delivery and Energy Reliability, "Smart grid." [Online]. Available: http://energy.gov/oe/technology-development/smart-grid

[4] C. Gellings, "The concept of demand-side management for electric utilities," *Proc. IEEE*, vol. 73, no. 10, pp. 1468–1470, Oct. 1985.

[5] H. Salehfar and A. Patton, "A production costing methodology for evaluation of direct load control," *IEEE Power Eng. Rev.*, vol. 11, no. 2, p. 64, Feb. 1991.

[6] Y.-Y. Hsu and C.-C. Su, "Dispatch of direct load control using dynamic programming," *IEEE Trans. Power Syst.*, vol. 6, no. 3, pp. 1056–1061, Aug. 1991.

[7] B. Ramanathan and V. Vittal, "A framework for evaluation of advanced direct load control with minimum disruption," *IEEE Trans. Power Syst.*, vol. 23, no. 4, pp. 1681–1688, Nov. 2008.

[8] M. Fahrioglu and F. Alvarado, "Designing incentive compatible contracts for effective demand management," *IEEE Trans. Power Syst.*, vol. 15, no. 4, pp. 1255–1260, Nov. 2000.

[9] H. Salehfar and A. Patton, "Modeling and evaluation of the system reliability effects of direct load control," *IEEE Trans. Power Syst.*, vol. 4, no. 3, pp. 1024–1030, Aug. 1989.

[10] P. Palensky and D. Dietrich, "Demand side management: Demand response, intelligent energy systems, and smart loads," *IEEE Trans. Ind. Informat.*, vol. 7, no. 3, pp. 381–388, Aug. 2011.

[11] P. Samadi, H. Mohsenian-Rad, R. Schober, and V. Wong, "Advanced demand side management for the future smart grid using mechanism design," *IEEE Trans. Smart Grid*, vol. 3, no. 3, pp. 1170–1180, Sep. 2012.

[12] N. Lu, "An evaluation of the HVAC load potential for providing load balancing service," *IEEE Trans. Smart Grid*, vol. 3, no. 3, pp. 1263–1270, Sep. 2012.

[13] K.-H. Ng and G. Sheble, "Direct load control—a profit-based load management using linear programming," *IEEE Trans. Power Syst.*, vol. 13, no. 2, pp. 688–694, May 1998.

[14] Staff Report, "Assessment of demand response and advanced metering," Federal Energy Regulatory Commission, Tech. Rep., Feb. 2011.

[15] E. H. Mathews, C. P. Botha, D. C. Arndt, and A. Malan, "HVAC control strategies to enhance comfort and minimise energy usage," *Energy Buildings*, vol. 33, no. 8, pp. 853–863, Oct. 2001.

[16] N. Nassif, S. Kajl, and R. Sabourin, "Evolutionary algorithms for multi-objective optimization in HVAC system control strategy," in *Proc. IEEE North Amer. Fuzzy Info. Proc. Soc. Annu. Meet. (NAFIPS)*, vol. 1, Banff, Canada, Jun. 2004, pp. 51–56.

[17] F. Calvino, M. La Gennusa, G. Rizzo, and G. Scaccianoce, "The control of indoor thermal comfort conditions: Introducing a fuzzy adaptive controller," *Energy Buildings*, vol. 36, no. 2, pp. 97–102, Feb. 2004.

[18] S. Ari, I. A. Cosden, H. E. Khalifa, J. F. Dannenhoffer, P. Wilcoxen, and C. Isik, "Constrained fuzzy logic approximation for indoor comfort and energy optimization," in *Proc. IEEE Fuzzy Info. Process. Soc. Annu. Meet.*, Jun. 2005, pp. 500–504.

[19] A. I. Dounis and C. Caraiscos, "Advanced control systems engineering for energy and comfort management in a building environment–A review," *Renew. Sust. Energy Rev.*, vol. 13, no. 6-7, pp. 1246–1261, 2009.

[20] *Thermal Environmental Conditions for Human Occupancy*, ASHRAE Std. 55-2010.

[21] M. Hamdi and G. Lachiver, "A fuzzy control system based on the human sensation of thermal comfort," in *Proc. IEEE World Congr. Comput. Intell.*, Anchorage, AK, May 1998, pp. 487–492.

[22] K. Chen, Y. Jiao, and E. S. Lee, "Fuzzy adaptive networks in thermal comfort," *Appl. Math. Lett.*, vol. 19, no. 5, pp. 420–426, 2006.

[23] J. Liang and R. Du, "Thermal comfort control based on neural network for HVAC application," in *Proc. IEEE Control Appl. Conf.*, Toronto, Canada, Aug. 2005, pp. 819–824.

[24] A. Faruqui and S. Sergici, "Household response to dynamic pricing of electricity: A survey of the empirical evidence," *J. Regulatory Economics*, vol. 38, pp. 193–225, Oct. 2010.

[25] A. Rogers, S. Maleki, S. Ghosh, and N. R. Jennings, "Adaptive home heating control through Gaussian process prediction and mathematical programming," in *Proc. Agent Technologies for Energy Systems*, Toronto, Canada, May 2010.

[26] R. T. Guttromson, D. P. Chassin, and S. E. Widergren, "Residential energy resource models for distribution feeder simulation," in *Proc. IEEE PES Gen. Meet.*, Toronto, Canada, 2003, pp. 108–113.

[27] D. P. Chassin, J. M. Malard, C. Posse, A. Gangopadhyaya, N. Lu, S. Katipamula, and J. V. Mallow, "Modeling power systems as complex adaptive systems," Pacific Northwest National Laboratory, Tech. Rep., December 2004.

[28] D. Hammerstrom et al., "Pacific Northwest GridWise testbed demonstration projects—part I: Olympic Peninsula project," U.S. Department of Energy at Pacific Northwest National Laboratory, Tech. Rep. PNNL-17167, Oct. 2007.

[29] P. Constantopoulos, F. C. Schweppe, and R. C. Larson, "ESTIA: A real-time consumer control scheme for space conditioning usage under spot electricity pricing," *Comp. Oper. Res.*, vol. 18, no. 8, pp. 751–765, 1991.

[30] D. J. Livengood, "The Energy Box: Comparing locally automated control strategies of residential electricity consumption under uncertainty," Ph.D. dissertation, Massachusetts Institute of Technology, Sep. 2011.

[31] D. Molina, C. Lu, V. Sherman, and R. Harley, "Model predictive and genetic algorithm based optimization of residential temperature control in the presence of time-varying electricity prices," in *Proc. IEEE Industry Applications Soc. Ann. Meet.*, Oct. 2011.

[32] A. Aswani, N. Master, J. Taneja, D. Culler, and C. Tomlin, "Reducing transient and steady state electricity consumption in HVAC using learning-based model-predictive control," *Proc. IEEE*, vol. 100, no. 1, pp. 240–253, Jan. 2012.

[33] F. I. Vázquez and W. Kastner, "Thermal comfort support application for smart home control," in *Ambient Intelligence - Software and Applications*, ser. Advances in Intelligent and Soft Computing, P. Novais, K. Hallenborg, D. I. Tapia, and J. M. C. Rodríguez, Eds. Springer Berlin / Heidelberg, 2012, vol. 153, pp. 109–118.

[34] R. Sonderegger, "Dynamic models of house heating based on equivalent thermal parameters," Ph.D. dissertation, Princeton University, 1978.

[35] U.S. Department of Energy at Pacific Northwest National Laboratory. GridLAB-D, power distribution simulation software. [Online]. Available: http://www.gridlabd.org/

[36] Residential module user's guide. GridLAB-D, power distribution simulation software. [Online]. Available: http://sourceforge.net/apps/mediawiki/gridlab-d/index.php?title=Residential_module_user's_guide

[37] ASHRAE, *2009 ASHRAE Handbook: Fundamentals*. ASHRAE, 2009.

[38] National Renewable Energy Laboratory. National Solar Radiation Data Base, Typical Meteorological Year 2. [Online]. Available: http://rredc.nrel.gov/solar/old_data/nsrdb/1961-1990/tmy2/

[39] ——. Solar Radiation Research Laboratory. [Online]. Available: http://www.nrel.gov/midc/srrl_bms/

[40] MISO. Market Reports. [Online]. Available: https://www.midwestiso.org/Library/MarketReports/Pages/MarketReports.aspx

[41] A. G. Thomas, C. Cai, D. C. Aliprantis, and L. Tesfatsion, "Effects of price-responsive residential demand on retail and wholesale power market operations," in *Proc. IEEE Power & Energy Soc. Gen. Meet.*, San Diego, CA, Jul. 2012.

[42] P. J. Antsaklis and A. M. Michel, *Linear Systems*. Boston: Birkhäuser, 2005.

[43] A. Takayama, *Mathematical Economics*, 2nd ed. Cambridge University Press, 1985.

[44] D. Kosterev, A. Meklin, J. Undrill, B. Lesieutre, W. Price, D. Chassin, R. Bravo, and S. Yang, "Load modeling in power system studies: WECC progress update," in *Power and Energy Soc. Gen. Meet.* Pittsburgh, PA: IEEE, Jul. 2008.

[45] K. Schneider and J. Fuller, "Detailed end use load modeling for distribution system analysis," in *Power and Energy Soc. Gen. Meet.* Minneapolis, MN: IEEE, Jul. 2010.

[46] K. Schneider, J. Fuller, and D. Chassin, "Analysis of distribution level residential demand response," in *Power Systems Conf. and Expos. (PSCE).* Phoenix, AZ: IEEE, Mar. 2011.

[47] Z. Zhou, F. Zhao, and J. Wang, "Agent-based electricity market simulation with demand response from commercial buildings," *IEEE Trans. Smart Grid*, vol. 2, no. 4, pp. 580–588, Dec. 2011.

[48] J. Fuller, K. Schneider, and D. Chassin, "Analysis of residential demand response and double-auction markets," in *Power and Energy Soc. Gen. Meet.* Detroit, MI: IEEE, Jul. 2011.

[49] A. G. Thomas, P. Jahangiri, D. Wu, C. Cai, H. Zhao, D. C. Aliprantis, and L. Tesfatsion, "Intelligent residential air-conditioning system with smart-grid functionality," to appear in *IEEE Trans. Smart Grid.*

[50] "Integrated retail/wholesale power system operations with smart grid functionality: Project homepage." [Online]. Available: http://www.econ.iastate.edu/tesfatsi/IRWProjectHome.htm

[51] AMES wholesale power market testbed homepage. [Online]. Available: http://www.econ.iastate.edu/tesfatsi/AMESMarketHome.htm

[52] GridLAB-D. Pacific Northwest National Laboratory (PNNL). [Online]. Available: http://www.gridlabd.org/

[53] K. P. Schneider, Y. Chen, D. P. Chassin, R. Pratt, D. Engel, and S. Thompson, "Modern grid initiative distribution taxonomy final report," Pacific Northwest National Lab, Tech. Rep., November 2008.

[54] K. Schneider, Y. Chen, D. Engle, and D. Chassin, "A taxonomy of North American radial distribution feeders," in *Power and Energy Soc. Gen. Meet.* Calgary, Alberta, Canada: IEEE, Jul. 2009.